# A Critical Review on Recent Advancements of the Removal of Reactive Dyes from Dyehouse Effluent by Ion-exchange Adsorbents

**Mohammad M. Hassan[1],[*] Christopher M. Carr[2]**

[1] *Food & Bio-based Products Group, AgResearch Limited, Private Bag 4749, Christchurch 8140, New Zealand.*

[2] *School of Design, University of Leeds, Leeds LS2 5JQ, United Kingdom.*

**Abstract**

The effluent discharged by the textile dyehouses has serious detrimental effect on aquatic environment. Some dyestuffs produce toxic decomposition products and the metal complex dyes releases toxic heavy metals to watercourses. Of the dyes used in the textile industry, effluents containing reactive dyes are the most difficult to treat because of the high water-solubility and poor absorption into fiber of these dyes. A range of treatments has been investigated for the decolorization of textile effluents and the adsorption seems to be one of the cheapest, effective and convenient treatments. In this review, the adsorbents investigated in the last decade for the treatment of textile effluent containing reactive dyes including

[*] Corresponding author. Tel.: +64-3-321-8755, fax: +64-3-321-8811
*E-mail address:* mahbubul.hassan@agresearch.co.nz

modified clays, biomasses, chitin and its derivatives, and magnetic ion-exchanging particles have been critically reviewed and their reactive dye binding capacities have been compiled and compared. Moreover, the dye binding mechanism, dye sorption isotherm models and also the merits/demerits of various adsorbents are discussed. This review also includes the current challenges and the future directions for the development of adsorbents that meet these challenges. The adsorption capacities of adsorbents depend on various factors, such as the chemical structures of dyes, the ionic property, surface area, and porosity of the adsorbents, and the operating conditions. It is evident from the literature survey that decolorization by the adsorption shows great promise for the removal of color from dyehouse effluent. If, biomasses want to compete with the established ion-exchange resins and activated carbon, their dye binding capacity will need to be substantially improved.

***Keywords***: Decolorization, dyehouse effluent, reactive dyes, adsorption, ion-exchange, magnetic

## 1. **Introduction**

Textile industries, more specifically chemical processing textile industries, are at a crossroad because of the stringent guidelines and consent limits set by environmental agencies in various developed and developing countries for discharging effluent containing dyes and chemicals to watercourses. Textile dyeing and printing industries are under scrutiny because they discharge colored effluents to watercourses that quite easily draw the attention of general public.

Most of the dyes used in the textile industry are not harmful as the leading dye manufacturers are no more manufacturing carcinogenic or hazardous dyestuffs. Sometimes it is not actually the dyes and auxiliaries themselves but their decomposition products become toxic. The color is the main factor for which textile dyehouse effluent needs treatment as the deep color of the effluent impairs the penetration of light through it affecting the photosynthesis reactions to produce oxygen in water by underwater plants and thereby affecting the viability of aquatic animals and plants [Lambert and Davy, 2011]. Some dyes are not biodegradable or have very low biodegradability. Dyes and auxiliaries increase the total dissolved solids content, total suspended solids content and also the chemical oxygen demand and biological oxygen demand of the effluent that negatively affects the aquatic ecological system. Some reactive dyes are metal complexed with copper, chromium, and nickel. When these dyes degrade, they release toxic heavy metals into the environment that can end up in the food chain. As reactive dyes are mainly used for the dyeing of cellulosic and protein fibers, it is necessary to observe the characteristics of cellulosic and protein fiber processing industry effluent. The treatment of dyehouse effluent containing the reactive dyes is the most problematic. The dyes in the effluent are in the non-reactive hydrolyzed state, highly soluble in water and their concentrations are high because of their low absorption into the fiber. Fig. 1 shows the chemical structure of several commonly investigated reactive dyes [Karcher et al., 2002].

Several reviews have been published in the area of removal of dyes from effluent by adsorption,[3–5] but they have targeted either a specific dye or a specific type of adsorbent. Some of these reviews are quite old and, in the meantime, many high performing adsorbents have been developed. None of the previous reviews specifically addressed the treatment of effluent containing reactive dyes (the most problematic of the dye classes used in textile industry) and compared the dye-binding capacities of various ion-exchange type adsorbents.

In this review, ion-exchange type modified clays, cellulosic and microbial biomasses, chitin and its derivatives, and magnetic particles with their reactive dye binding capacities, have been compiled, presented and compared.

## 2. Types of ion-exchange adsorbents

The ion-exchange adsorbents imply by name that they bind pollutants of opposite charge. As the reactive dyes are anionic, only anion-exchanging adsorbents have been covered in this review. A range of adsorbents, such as clay, ion-exchange resins, lignocellulosic biomasses, protein biomass, microbial biomasses, have been investigated for the removal of color from reactive dye effluent [Yagub et al., 2014, Bharathi and Ramesh, 2013].

### *2.1. Clay type adsorbents and their dye binding performance*

#### *2.1.1. Clay adsorbents*

The type of clays, especially those that are rich in iron and aluminum, can be used for the removal reactive dyes from the effluent. Some of the clay-type adsorbents are synthetically made (e.g. layered double hydroxides), while others are waste products of industrial processing (e.g. red mud). Both calcined and non-calcined types of clays have been investigated for the removal of reactive dyes but the calcined clays are preferred over non-calcined clays due to their higher surface area and also they show better dye binding capacity. The clay-like materials investigated for the removal of reactive dyes include nano-hydroxyapatite [Kyzas et al., 2013], layered double hydroxides (LDH) [Sumari et al., 2016,

Aguiar et al., 2013, Asouhidou et al., 2012], $Mg(OH)_2$-modified-kaolin [Amin et al., 2015], and also the sea-water neutralized and calcined red mud [de Jesus et al., 2015, de Souza et al., 2013, Wang et al., 2009]. The laccase-modified fumed silica [Kalkan et al., 2014], nano-alumina [Nadafi et al., 2014], zinc and magnesium oxide nanoparticles [Khoshhesab et al., 2015, Venkatesha et al., 2012], kaolinite and smectite [Errais et al., 2012], $Mg(OH)_2$-coated bentonite [Chinoune et al., 2016], silylated palygorskite [Xue et al., 2010], and synthetic talc [Rahman et al., 2013] also can be included in this list of clay-like materials.

*2.1.2. Reactive dye binding capacity of clay-like adsorbents and dye binding mechanisms*

The dye binding capacities and operating conditions of removal of reactive dyes by clay-like adsorbents are shown in Table S1 (Supplementary Information). Raw kaolinite, synthetic talc, and Fouchana clays show quite meager reactive dye binding capacity. On the other hand, laccase modified fumed silica, seawater-neutralized red mud calcined at 500 °C, and calcined Mg/Al LDH showed quite good dye binding capacity. Of the clays investigated, non-calcined Mg/Al LDH showed the highest reactive dye binding capacity for the removal of C.I. Reactive Blue 4 (328.9 mg $g^{-1}$).

*2.1.3. Reactive dye binding mechanisms*

Fig. 2 shows the chemical structure of a few clay-type adsorbents and their reactive dye binding mechanisms. Aluminum and iron are tri and di or trivalent metals respectively with positive charges and therefore aluminum and iron-rich clays can electrostatically bind anionic reactive dyes. Some of these clays, such as $Mg(OH)_2$-coated bentonite and silylated palygorskite, have hydroxyl groups on their surface that can bind hydroxyl and amino groups containing reactive dyes through hydrogen bonding and Van der Waals forces. Laccase is a

protein enzyme, therefore, laccase-modified clays can electrostatically bind anionic reactive dyes.

### *2.1.3. Merits and demerits*

The advantage of clay-type adsorbents may include their very good hydrodynamic properties and also they are cheap. However, their dye-binding capacity is not comparable to ion-exchange resins and therefore they cannot be alone effective for the complete removal of dyes from effluent.

## *2.2. Ion-exchange resins*

Ion-exchange resins are polymeric granules or beads with various functional groups that are capable of binding ions of opposite charge. They are either cation-exchange or anion-exchange resin.

### *2.2.1. Commercial anion-exchange resins*

They are the first generation adsorbents developed for the removal of dyes from textile effluent when the color of effluent became an issue around the world. A range of anion-exchange resins, such as zeolite-based Macrosorb (Crossfield), and synthetic organic polymer-based S6328 (Bayer), MP62 (Bayer), Amberlite IRC-71 (Dow), and Dowex (Dow), are commercially available. Of them, S6328 and MP62 [Low and Lee, 1997], and also Amberlite IRC-71 [Karcher et al., 2002], have been investigated for the removal of reactive dyes.

138

139 *2.2.2. Non-commercial anion-exchange resins*

140 A range of ion-exchange resins, such as poly(acrylic acid-N-isopropylacrylamide-
141 trimethylolpropanetriacrylate) cross-linked with sodium alginate [Dhanapal and
142 Subramanian, 2014], partial diethylamino-ethylated cotton dust waste [Fontana et al., 2016],
143 quaternized wood [Low et al., 2000], microcrystalline cellulose gel [El-Naggar et al., 2018],
144 quaternized flax cellulose [Ma and Wang, 2015], cucurbit[6]uril and cucurbit[8]uril [Xie et
145 al., 2016], porous chitosan-polyaniline/ZnO hybrid composite [Kannusamy and Sivalingam,
146 2013], and quaternized sugarcane bagasse [Wong et al., 2009, Aly et al., 2018], have been
147 investigated as candidate adsorbents for the removal of reactive dyes from dyehouse effluent.
148 Some other ion-exchange resins that are worthy to mention may include ethylenediamine
149 functionalised and potassium fluoride activated paper sludge [Auta and Hameed, 2014],
150 poly(AA-NIPAAm-TMPTA) cross-linked with sodium alginate [Dhanapal and Subramanian,
151 2014], cellulose nanocrystal-reinforced keratin [Song et al., 2017], starch/polyaniline
152 nanocomposite [Janaki et al., 2012], α-cellulose/polypyrrole [Ovando-Medina et al., 2015],
153 hollow zein nanoparticles [Xu et al., 2013], lignin chemically modified with aluminum and
154 manganese [Adebayo et al., 2014] , and epichlorohydrin (ECH)-cross-linked chitosan
155 nanoparticles [Chen et al., 2011].

156

157 *2.2.3. Reactive dye removal performance of ion-exchange resins*

158 Table 1 shows reactive dye binding capacity of various ion-change resins investigated for
159 the removal of reactive dyes from dyehouse effluent. The commercial ion-exchange resins
160 investigated for this purpose are Bayer anion exchange resins S6328 and MP62, and also SR
161 Amberlite IRC-718 [Karcher et al., 2002, Low and Lee, 1997]. Of them, Amberlite IRC-718
162 showed very poor dye binding capacity for the C.I. Reactive Blue 2 and C.I. Reactive Orange

16 [Karcher et al., 2002]. The Bayer MP62 anion-exchange resin showed excellent binding of C.I. Reactive Black 5 dye as the dye binding capacity reached 1190.14 mg $g^{-1}$ [Low and Lee, 1997]. However, for the same dye, the Bayer S6328a ion-exchange resin showed only half of the dye binding capacity compared to the MP62 resin. Of the non-commercial resins investigated, quaternized rice husk, acid burnt silk cotton hull, and cationic polyelectrolyte poly(epichlorohydrin-dimethylamine) modified bentonite showed quite inadequate reactive dye binding capacity. However, cellulose nanocrystal-modified keratin and hollow zein nanoparticles showed excellent removal of various reactive dyes from effluent and their reactive dye binding capacity was comparable to the commercial Bayer MP62 ion-exchange resin. Thus, it will not be an exaggeration to say that some of the ion-exchange resins developed over the years can compete with commercial ion-exchange resins. From Table 1, it is evident that except cucurbit[6]uril, cucurbit[8]uril, quaternized flax cellulose, partial diethylamino-ethylated cotton dust waste, and acid burnt silk cotton hull and MP62, all other investigated adsorbents including the high performing MP62, cellulose crystal modified with keratin and hollow zein nanoparticles showed the maximum reactive dye binding capacity at highly acidic conditions. It is unfavorable as the pH of dyehouse reactive dyeing effluent is usually 7-11. The pH of the effluent will need to be reduced to that level by using strong acids and after the decolorization treatment, the treated effluent will need to be neutralized by adding alkali.

### *2.2.3. Merits and demerits of ion-exchange resins*

The ion-exchange resins are easy to handle and they can be easily recycled and reused. However, commercially available ion-exchange resins are relatively expensive and therefore a range of cheap alternatives, such as unmodified and modified cellulosic biomasses, have been extensively explored as an alternative to commercial ion-exchange resins. Ion-exchange

resins are very popular, but their disposal is a problem as the synthetic ion-exchange resins are not biodegradable.

### *2.3. Biomass-based absorbents and their dye binding performance*

Biomasses are renewable organic polymeric materials, such as plants or plant-based materials, wood, agricultural wastes, dead microbes, and material of animal origin. Biomasses can be divided mainly into two categories, namely (1) lignocellulosic, and (2) proteinous. The protein biomasses could be plant, animal or microorganism-based but the lignocellulosic biomasses are usually plant-based. Various types of biomasses, lignocellulosic and microbial, have been investigated as adsorbents for the removal of reactive dyes.

#### *2.3.1. Cellulosic biomasses and their reactive dye binding capacity*

A large number of lignocellulosic biomasses, such as raw agricultural solid wastes (e.g. leaves, fibers, fruit and peel, and waste materials), have been investigated as adsorbents for binding reactive dyes. The investigated solid wastes are the fruit and peel of *Trapa bispinosa*, grape fruit peel [Abassi et al., 2009], alfa fibers [Fettouche et al., 2015], Bengal gram seed husk [Reddy et al., 2017], soybean stalk, hulk and residue [Honorio et al., 2016, Gao et al., 2015, Ashori et al., 2014], eucalyptus bark [Moraisi et al., 1999], pomelo peel [Argun et al., 2014], peanut hull [Tanyildizi et al., 2011], hazelnut shell [Ferrero,2007], Brazilian pine fruit coat [Lima et al., 2008], modified wallnut shell [Cao et al., 2014], cupuassu shell [Cardoso et al., 2011a], *P. oceanica* leaf sheaths [Ncibi et al., 2007], Aqai palm (*Euterpe oleracea*) stalk [Cardoso et al., 2011b], Brazilian pine fruit shell [Cardoso et al., 2011c], pomegranate seed

powder [Ghaneian et al., 2015], and waste products from forest industries including wood, bark, and sawdust [Ratnamala et al., 2016, Chakraborty et al., 2006]. These materials are abundantly available in large quantities at a very cheap price, and they could be potential dye adsorbents because of their unique physicochemical characteristics.

Table 2 shows the adsorption performance of various reactive dyes by lignocellulosic biomasses. Of the cellulosic biomasses investigated, municipal solid waste compost, alpha fiber powder, soybean stalk powder, grapefruit peel and cupuassu shell showed very poor reactive dye binding capacity. On the other hand, modified walnut shell and soybean residue showed fairly good dye binding capacity. The investigation of operating conditions on the dye binding capacity shows that almost all of the cellulosic biomasses show the maximum absorption at strongly acidic pH. The reactive dyes are removed by forming hydrogen bonds with hydroxyl groups of these constituents and also through Van der Waals forces.

224224

*2.3.2. Chitosan and its derivative*

Chitosan, a waste product of the seafood industry, also has been extensively investigated as a candidate adsorbent for the removal of reactive dyes. Chitosan has been investigated as fine powder [Ignat et al., 2012, Annadurai et al., 2008], porous particles [Jiang et al., 2014, Chiou et al., 2002], flakes [Filipkowska, 2006], and films [Nga et al., 2017], for the removal of dyes. Chitin-rich squid pens have also been investigated for the removal of reactive dye [Figueiredo et al., 2000]. However, mixed results were reported for the reactive dye binding capacity of chitosan, as the dye binding capacity depends on the source and also on its molecular weight. A commercial chitosan powder showed poor dye removal but another chitosan powder made from an Indian shrimp showed the excellent removal of reactive dyes [Subramani and Thinakaran, 2000]. Various chitosan derivatives, such as ECH-cross-linked

chitosan nanoparticles [Chen et al., 2011], ECH-cross-linked chitosan beads [Chiou et al., 2004], cross-linked chitosan, chitosan cross-linked with sodium edetate [Jóźwiak et al., 2015], cross-linked quaternized chitosan [Rosa et al., 2008], 3-aminopropyl-7-triethoxysilane modified chitosan beads [Vakili et al., 2015], polyethyleneimine-grafted-chitosan beads [Chatterjee et al., 2011], epichlorohydrin-cross-linked chitosan beads [Kim et al., 2012, Chiou et al., 2003], and poly(acrylamide)-grafted-chitosan [Kyzas and Lazaridis, 2009], also have been investigated as an adsorbent.

*Reactive dye binding performance of chitosan derivatives*

Table 3 shows the dye binding capacity of virgin chitosan and its derivatives. Of them, chitosan cross-linked with epichlorohydrin showed an excellent removal of C.I. Reactive Black 5 and C.I. Reactive Orange 16 dyes as the dye binding capacity reached 5572.0 and 5392 mg $g^{-1}$ respectively [Vakili et al., 2015], almost four times of the dye binding capacity shown by the high-performing commercial Bayer MP62 ion-exchange resin. The same adsorbents also showed the excellent removal of C.I. Reactive Red 189 and C.I. Reactive blue 2 dyes [Chiou et al., 2002, Chiou et al., 2004], and the maximum removal of dyes occurred at pH 2, similar to the removal of reactive dyes by the MP62 resin. Chitosan cross-linked with sodium edetate also showed reasonably high dye binding capacity and the maximum removal occurred at pH 4 [Jóźwiak et al., 2015]. It is evident that unmodified chitosan showed the maximum dye binding at near to neutral pH but the chemically modified chitosan showed the maximum binding at highly acidic conditions.

*2.3.3. Color removal by microbial biomasses*

Microbial biomasses, dead or living, have been extensively investigated for the removal of reactive dyes in the effluent. Microbial biomass can include bacteria, fungi, and micro-algae. They can absorb dye molecules or the enzymes secreted by them can degrade chromophores of dye molecules causing their decolorization. The investigated bacteria are *E. coli* [Kim et al., 2016], *Nostoc linckia* [Mona et al., 2011], *Lemna gibba* [Guendouz et al., 2016], *Corynebacterium glutamicum,* and *Corynebacterium glutamicum* discharged from an industrial lysine fermentation plant [Won et al., 2008, Vijayaraghavan and Yun, 2007, Won et al., 2006], a mixture of *Alcaligenes faecalis* and *Commomonas acidovorans* [Oxspring et al., 1996], *Paenibacillus azoreducens* sp. nov. [Meehan et al., 2001], *Pseudomonas luteola*,[Chang et al., 2001],[Chang et al., 2000] *Lysinibacillus sp.*, and *Desulfovibrio desulfuricans* [Kim, 2007], and *Pseudomonas luteola* free cells [Hu, 1996]. Other than unmodified bacteria, esterified bacteria and *Lysinibacillus sp.*-attached electrospun polysulfone mat [San Keskin et al., 2015], have also been investigated as an adsorbent.

A range of fungi, including dead wood-rotting fungus (*Trametes versicolor*) [Binupriya et al., 2007], *Rhizopus arrhizus* [Aksu and Cagatay, 2006, Aksu and Tezer, 2000], *Aspergillus parasiticus* [Akar et al., 2009], *Thamnidium elegans* [Akar et al., 2017], fungal strain VITAF-1 [Sinha and Osborne, 2016], *Rhizopus nigricans* [Kumari and Abraham, 2007], *Penicillium ochrochloron* [Aytar et al., 2016], *Rhizopus nigricans* and *Penicillium restrictum* [Iscen et al., 2007], *Termitomyces clypeatus* [Bagchi and Ray, 2015], *Aspergillus versicolor* [Kara et al., 2012], *Aspergillus niger* [Bagchi and Ray, 2015] and *Symphoricarpus albus* [Kara et al., 2012], mixed *Aspergillus versicolor* and *Rhizopus arrhizus* with dodecyl trimethylammonium bromide,[Gül and Dönmez, 2013] *Phanerochaete chrysosporium*,[Dharajiya et al., 2016] *Aspergillus fumigatus*,[Dharajiya et al., 2016] mixed cultures isolated from textile effluent,[Çetin and Dönmez, 2006] and *Aspergillus fumigatus* isolated from textile effluent,[Karim et al., 2017] have been investigated as a candidate adsorbent for the removal

of reactive dyes. Also, several algae, including *Spirulina platensis*,[Cardoso et al., 2012] *Enteromorpha prolifera* [Sun et al., 2013], and *Chlorella vulgaris* [Aksu and Tezer, 2005], have been investigated for the removal of reactive dyes.

*Dye binding capacities of microbial biomasses*

Table S2 (Supplementary Content) shows the list of bacteria investigated for the removal of color and their dye absorption performance. Mona et al. investigated *Nostoc linckia* bacterium for the removal of C.I. Reactive Red 120 and found that absorption carried out at 35 °C showed higher dye absorption (422.5 mg $g^{-1}$) compared to the absorption carried out at 25 °C [Mona et al., 2011]. Some of the bacteria investigated for the decolorization of reactive dyes, such as *Lemna gibba* [Guendouz et al., 2016], and *Escherichia coli*[Kim et al., 2016], showed quite poor dye removal at as low as 6.13 mg $g^{-1}$ [Guendouz et al., 2016]. On the other hand, raw and esterified *E. coli*[Guendouz et al., 2016], and *Corynebacterium glutamicum* [Kim et al., 2016], showed excellent reactive dye binding capacity. Most of the bacteria investigated showed the highest dye binding capacity at pH 1-3 [Akar et al., 2017, Sinha and Osborne, 2016], except *Pseudomonas luteola* free cells and *Desulfovibrio desulfuricans*. They showed the maximum removal at neutral to alkaline pH.

Of the fungi investigated, *Aspergillus versicolor*, *Termitomyces clypeatus*, *Aspergillus niger*, and *Symphoricarpus albus* showed relatively poor reactive dye binding capacity. However, VITAF-1 and *Rhizopus nigricans* showed quite good dye binding capacity. Unlike bacteria, fungi show their dye binding capacity at a broad pH (1-8) [Aytar et al., 2016, Gül and Dönmez, 2013, Dharajiya et al., 2016]. All of the fungi showed quite a poor removal of the dye except *Rhizopus arrhizus* and VITAF-1. Of the fungal biomasses, *Rhizopus* (*Rhizopus arrhizus*) showed the highest reactive dye binding capacity for both C.I. Reactive Black 5 and

C.I. Reactive Blue 21 dyes (501 and 773 mg $g^{-1}$ respectively) when the treatment was carried out at 35 and 45 °C respectively at pH 2. Won et al. investigated *Rhizopus oryzae* in combination with *Aspergillus versicolor* with or without cetyltrimethylammonium bromide (CTAB) for the removal of C.I. Reactive Blue 19, but found that 100% decolorization took 6 days when the decolorization treatment was carried out in the presence of CTAB [Won et al., 2006]. Without CTAB, the color removal efficiency dropped to 86% for the same time period. Other than bacteria and fungi, microalgae also have been investigated as adsorbents. Of them, *Spirulina platensis* [Cardoso et al., 2012], and *Enteromorpha prolifera* [Sun et al., 2013], showed some levels of reactive dye binding capability. Although *Chlorella vulgaris* showed quite a good removal of C.I. Reactive Black 5, for the C.I. Reactive Orange 107 the binding capacity was very poor [Aksu and Tezer, 2005].

*Adsorption mechanisms of microbial biomasses*

The adsorption of dyes onto lignocellulosic adsorbents occurs mainly by the ionic interactions between the anionic sulfonate groups of dyes and the cationic amino or quaternary ammonium groups of adsorbents. However, the removal of color by bacterial cells mainly occurs by the physical adsorption of dye molecules into bacterial cells [Bras et al., 2001]. The color removal efficiency is diffusion dependent, and when the surface of a cell is saturated with dye molecules, the adsorption of dye molecules stops. The disadvantages of bacterial biomass adsorption based treatments include the difficulty of removing the adsorbents from the treated water, and also recovered biomass will need to be disposed of. Therefore, degradation of the dyestuffs could be favorable as they permanently remove the color. Reactive dyes are quite large molecules and also have substituent sulfonate groups. Therefore, reactive dye molecules will be unlikely absorbed into the cells by passing through

the cell membrane and therefore the dye removal is not dependent on the intracellular uptake of the dye [Robinson et al., 2001]. The adsorbed dye could be reduced by enzymes (such as cytoplasmic flavin-dependent azoreductases) produced by bacterial cells [Robinson et al., 2001]. Pearce et al. opine that electron transport-linked reduction could be responsible for the reduction of dyes in the extracellular environment [Pearce et al., 2003]. During the metabolism of the certain substrate, bacteria form low molecular weight redox mediator compounds that can act as electron shuttles between the azo dye and a nicotinamide adenine dinucleotide (NADH)-dependent azoreductase that is available in the outer membrane [Gingell and Walker, 1971]. In an anaerobic condition, the addition of anthraquinone sulphonate can facilitate the non-enzymatic reduction of azo chromophores [Plumb et al., 2001]. Therefore, the removal of dyes by bacteria could be a combination of adsorption and reduction process. The removal of color by microbial biomasses is advantageous as the absorbed dyes are degraded unlike any other type of adsorbent.

### *2.3.4. Merits and demerits of biomass adsorbents*

The main advantages of biomass-based adsorbents may include their easy disposal because of their high biodegradability and low cost. However, the poor dye binding capacities shown by various cellulosic biomasses indicates that they cannot compete with the commercial ion-exchange resins. The main constituents of cellulosic biomass are cellulose, hemicellulose, lignin, and polyphenols and all of them are weakly anionic. Because of their weakly anionic nature, cellulosic adsorbents are not a good adsorbent for the removal of anionic reactive dyes. On the other hand, chitosan is cationic and therefore it can bind reactive dyes by forming ionic bonding. It can be concluded that cross-linked and quaternized chitosan derivatives are promising adsorbents that can replace commercial ion-exchange

resins for the removal of reactive dyes from the effluent. However, the use of chitosan as a dietary supplement has increased its price. The key challenges of removal of dyes by biosorption are the difficulties in procurement and transportation of high volume of biomasses, poor hydrodynamic properties, poor recyclability and their removal from the treated effluent.

### *2.4. Magnetic ion-exchange adsorbents and their reactive dye binding performance*

#### *2.4.1. Magnetic ion-exchange adsorbents*

The high removal of color by an adsorbent is not enough, as the separation of biosorbent from the treated water is cumbersome. Therefore, recent research has emphasized on the ease of separation of adsorbent from the treated effluent, resulting in the development of magnetic nanoparticles. By using a strong magnet, the used adsorbent can be easily separated. The investigated magnetic nanoparticles may include laccase immobilized epoxy-functionalized magnetic chitosan beads [Bayramoglu et al., 2010], magnetic chitosan microparticles functionalised with polyamidoamine dendrimers [Wang et al., 2015], magnetic N-lauryl chitosan particles [Debrassi et al., 2012], glutaraldehyde (GLA) cross-linked magnetic chitosan nanoparticles [Elwakeel et al., 2009], chitosan-based magnetic microspheres [Xu et al., 2018], glutaraldehyde cross-linked magnetic chitosan nanocomposites [Kadam and Lee, 2015], modified magnetic chitosan microspheres [Jafari et al., 2016], quaternized magnetic resin microspheres [Li et al., 2014], magnetic carbon nanotube-κ-carrageenan-$Fe_3O_4$ nanocomposite [Duman et al., 2016], quaternized magnetic microspheres [Shuang et al., 2012], O-carboxymethyl chitosan-N-lauryl/γ-$Fe_2O_3$ magnetic nanoparticles [Demarchi et al., 2015], L-arginine-functionalized $Fe_3O_4$ nanoparticles [Dalvand et al., 2016], and magnetic

$Fe_3O_4$/chitosan nanoparticles [Cao et al., 2015]. The nanoparticles are mostly made magnetic by forming either $Fe_2O_3$ or $Fe_3O_4$ nanoparticles in-situ within the organic or inorganic nanoparticles.

383383

*2.4.2. Reactive dye binding capacity and dye binding mechanisms*

Table 4 shows the reactive dye binding capacity of various organic magnetic nanoparticles investigated as a candidate adsorbent for the removal of reactive dyes from the effluent. Of the magnetic nanoparticles investigated, only a few of them show some levels of potential as adsorbents. Of them, laccase immobilized magnetic chitosan beads showed very poor dye-binding capacity as the adsorbent showed only 2.05 and 1.42 mg $g^{-1}$ dye adsorption in the case of C.I. Reactive Yellow 2 and C.I. Reactive Blue 4 respectively. Magnetic carbon nanotube-κ-carrageenan-$Fe_3O_4$ nanocomposite also showed relatively low dye binding capacity but considerably higher than the dye binding capacity shown by laccase immobilized magnetic chitosan beads. Of the magnetic nanoparticles investigated, quaternized magnetic resin microspheres and quaternized GLA-cross-linked magnetic chitosan particles showed some reasonable levels of dye binding capacity, 773.6 and 936.6 mg $g^{-1}$ for the C.I. Reactive Black 5 and C.I. Reactive Red 120 dyes, respectively at highly acidic conditions (pH 2) [Elwakeel et al., 2009, Shuang et al., 2012]. It is evident that the formation of magnetic nanoparticles within the pores of organic micro/nanoparticles substantially reduces their porosity and pore volume, which affects their dye binding performance, as the magnetic particles of chitosan showed much lower dye binding capacity compared to the ECH-cross-linked chitosan. They are not practical for the removal of dyes as the cost of production of these adsorbents will be relatively high and the levels of removal achieved are only one-third of the dye binding capacity shown by activated carbon. The challenges of magnetic nanoparticles are the non-availability of these adsorbents at an economical price, low reactive

dye binding capacity, poor decolorization efficiency and the economic regeneration of the adsorbents.

The magnetic ion-exchange adsorbents bind dye molecules having opposite charge and also can bind dye molecules having hydroxyl and amino groups through hydrogen and van dar Waal's bonding.

### *2.4.4. Merits and demerits of magnetic ion-exchange adsorbents*

The key advantage of magnetic ion-exchange adsorbents is their easy removal from the treated effluent. However, they show relatively poor dye binding capacity compared to the other adsorbents investigated.

## 3. Effect of functional and substituent groups on dye adsorption capacity

The reactive dyes have one or more than one anionic groups (usually sulfonic acid groups) and also some dyes have substituent groups, such as alkyl, amino, and acetamide groups. They may have an effect on their adsorption by ion-exchange type adsorbents. Auta and Hameed investigated the removal of two reactive dyes, C.I. Reactive Orange 16 and also C.I. Reactive Blue 19 by the functionalized paper sludge [Auta and Hameed, 2014]. Both of the dyes have two sulfonic acid groups in their structure but the removal of C.I. Reactive Orange 16 dye was better than the other dye, which has a cationic amino functional group. The cationic substituent group affected its absorption by the activated paper sludge. Starch aniline composites have been investigated for the removal of C.I. Reactive Black 5 and C.I. Reactive Violet 4 [Janaki et al., 2012]. The removal of four sulfonate groups-containing C.I. Reactive Black 5 was considerably better than the other dye which has three sulfonate groups and a hydrophobic acetamide group that affected its adsorption into the cationic starch adsorbent.

Similarly, in the case of sodium edetate cross-linked chitosan, the adsorption of six sulfonate groups-containing C.I. Reactive yellow 84 was 50% higher than the four sulfonate groups containing C.I. Reactive Black 5 [Jóźwiak et al., 2015]. In the case of ECH-cross-linked chitosan, four sulfonate groups-containing C.I. reactive Black 5 showed better adsorption than the two sulfonate groups-containing C.I. Reactive Orange 16. However, in the case of nanoporous (pore size = 2.9 nm) quaternized magnetic resin microparticles, six sulfonate groups-containing C.I. Reactive Red 120 absorbed less than two-sulfonate groups containing C.I. Reactive orange 16 [Shuang et al., 2012]. The molecular weight of C.I. Reactive Orange 16 is 617.526 but the molecular weight of C.I. Reactive Red 120 is 1469.98, more than double of the molecular weight of the other dye. The high molecular weight of C.I. Reactive Red 120 affected its adsorption into the nanoporous magnetic resin particles. Therefore, it is evident that the reactive dye adsorption by various ion-exchange type adsorbents is affected not only by the number of anionic groups in the dye but also by their molecular weight and the substituent groups present in the dye molecules.

## 4. Synthesis of anion-exchange resins

Anion-exchange resins can be produced by various methods including chemical modifications, polymeric grafting and also by crosslinking as mentioned below:

### *4.1. Homopolymerization and crosslinking*

In this case, cationic monomers are homo-polymerized and then cross-linked to form water-insoluble anion-exchange resins. Quaternary ammonium, polyamine, etc., are popular

polymers for making this kind of anion-exchange resins. Mainly two types of polymerization reactions, condensation and addition polymerization, are used to synthesize ion-exchange resins. For example, chitosan beads are prepared by using various crosslinking agents including covalent bond forming glutaraldehyde and epichlorohydrin and ionic bond, forming tripolyphosphate and sodium edetate. Fig. 3 shows the crosslinking of chitosan by using covalent bond forming epichlorohydrin and glutaraldehyde crosslinking agents as well as the ionic crosslinking with sodium edetate and trisodium citrate.

### *4.2. Copolymerization*

In this case, two types of monomers (monomers containing mono and divinyl groups) are copolymerized, which produces a random cross-linked copolymer. Cation-exchange and anion-exchange both types of ion-exchange resins can be produced by this method. A cation-exchange resin usually contains sulfonic and carboxylic acid groups, such as poly(styrene sulfonate-co-vinyl benzene) cation-exchange resin, which is produced by the free-radical copolymerization of styrene with divinylbenzene followed by sulfonation with sulfuric acid ($H_2SO_4$) as shown in Fig. 4. On the other hand, an anion-exchange resin usually contains amine or quaternary ammonium groups, such as poly(vinyl benzyl trimethyl-ammonium chloride-co-vinyl benzene) anion-exchange resin, which is produced by the free-radical copolymerization of (vinyl benzyl)trimethylammonium chloride with divinylbenzene (Fig. 4).

### *4.3. Crosslinking of two or more polymers.*

In this method, two or more polymers are cross-linked to form water-insoluble ion-exchange resins. The polymers used for making anion-exchange resins are mostly quaternary ammonium, polyamines, or other polymers having a primary, secondary, and/or tertiary amine groups. The polymers used for making cation-exchange resins contain carboxylic and sulfonic acid groups.

### *4.4. Chemical modification of polymers*

The polymers having hydroxyl, carboxyl, thiol or amino groups can be easily converted into an anion-exchange resin by chemical modifications. For example, sugarcane bagasse is a cellulosic material, which can be converted quaternary cellulose by reacting with a quaternary ammonium compound, such as 2,3-epoxypropyltrimethylammonium chloride [Hassan, 2014]. Fig. 5 (top) shows the mechanism of formation of quaternary ammonium chitosan and cellulose by reacting with an epoxy group-containing quaternary ammonium compound. The quaternary ammonium groups are strongly cationic and therefore they can act as an anion-exchange resin.

### *4.5. Polymeric grafting*

Graft-copolymerization is an important tool to modify the surface functionalities to make them either cationic or anionic, which is used to modify various lignocellulosic and carbonaceous adsorbents. Cationic polymers (e.g. polymers containing amine or quaternary ammonium groups, polyaniline, polypyrrole) are grafted onto cellulose macromolecular chain to introduce cationic functionalities to make them anionic-exchange resin. Cellulosic

materials contain a large number of hydroxyl groups (they are weakly anionic) and therefore it is advantageous to make them anionic exchange resin as the unsubstituted hydroxyl groups also will take part in the anion exchange. On the other hand, if a cellulosic material is converted into the anion-exchange resin, these unsubstituted hydroxyl groups will have a negative impact on their cationic exchange. For example, Fig. 5 (bottom) shows the formation of quaternized chitosan and cellulose by grafting a quaternary ammonium polymer onto their macromolecular chains [Hassan, 2015].

## 5. Modeling of adsorption process

### *5.1. Modeling of adsorption isotherm*

Adsorption of reactive dyes by various adsorbents can be expressed by various isotherm models. Adsorption isotherms are used to describe the interaction between the dye molecules, dye adsorption equilibrium, and the dye binding active sites of the adsorbents [Cao et al., 2015]. Adsorption isotherm expresses the amount of adsorbate on the absorbent surface as a function of its concentration at a constant temperature. Adsorption process of dyes can be described by various empirical adsorption isotherm models including Langmuir, Freundlich, Temkin, Dubinin–Radushkevich, Sips, Vieth–Sladek, Brouers–Sotolongo, and Radke–Prausnite. They are used to predict the adsorption capacities of reactive dyes by activated carbon and to fit the experimental equilibrium data. According to Freundlich model, adsorption takes place at specific heterogeneous surfaces and the linear form of this model is represented as [Freundlich, 1906, Vijayaraghavan et al., 2006]:

–

where $K_F$ (l $g^{-1}$) and n (dimensionless) are Freundlich isotherm constants which represent the adsorption and the degree of nonlinearity between solution concentration and adsorption, respectively. A plot of ln $q_e$ vs ln $C_e$ would result in a straight line with a slope of 1/$n$ and intercept of ln $K_F$. The Temkin isotherm model, like Freundlich model, is one of the earliest isotherm models, which was developed to describe the adsorption of hydrogen atom onto platinum electrodes in an acidic aqueous solution. In the Temkin adsorption isotherm equation, the energy of adsorption is a linear function of surface coverage. This adsorption model is only valid for medium ion concentrations. The linear form of the model is as follows [[Samarghandi et al., 2009]]:

— —

where b is a Temkin constant which is related to the heat of sorption (J $mol^{-1}$) and $K_T$ is a Temkin isotherm constant (l $mg^{-1}$) [Langmuir, 1916]. On the other hand, Langmuir model is based on four assumptions: all of the adsorption sites are equivalent and each site can only accommodate one molecule, the surface is energetically homogeneous and adsorbed molecules do not interact, there are no phase transitions, and at the maximum adsorption, only a monolayer is formed [Dubinin and Radushkevich, 1947]. Adsorption only occurs on localized sites on the surface, not with other adsorbates. The linear form of the Langmuir model can be represented as:

— —— ——— — [3]

The Dubinin–Radushkevich model has been widely used to correlate adsorption isotherms following a pore filling mechanism on activated carbons and other microporous adsorbents [Redlich and Peterson, 1959]. Other previous models could not accurately describe the adsorption of adsorbate into microporous adsorbents. The linear form of the model can be represented as:

547547

—

548548 where $q_s$ (mg P $g^{-1}$) is constant in the Dubinin–Radushkevich model, which is related to the
549549 absorption capacity. $K_D$ ($mol^2$ $kJ^{-2}$) is a constant related to the mean free energy of the
550 absorption

551 The Redlich-Peterson (R-P) isotherm is a three-parameter empirical adsorption model that
552 incorporates elements from both the Langmuir and Freundlich isotherms and improves the
553 inaccuracies [Sips, 1948]. The adsorption mechanism is unique, which does not follow ideal
554 monolayer adsorption characteristics. The linear form of the isotherm model can be expressed
555555 as:

556556 —

557 Sips model is a three-parameter isotherm model, which is combined a form of Freundlich
558 and Langmuir expressions deduced for predicting the heterogeneous adsorption [Gunay et al.,
559 2007]. The linear form of the model can be expressed as [Toth, 1971]:

—

560 Toth model is another three-parameter isotherm model developed to improve Langmuir
561 isotherm fittings, which is useful in describing heterogeneous adsorptions systems
562 [Lagergren, 1898]. The linear form of the model can be described as:

563 — –

564 The adsorption of reactive dyes by ion-exchange adsorbents can be described by using
565 Freundlich and Langmuir models. However, the adsorption of dyes by various adsorbents
566 mainly follows Langmuir and Freundlich isotherm models. For example, the adsorption of
567 reactive dyes by ion-exchange type adsorbents is mainly represented by the Langmuir

isotherm model and the kinetic data usually follow the pseudo-second-order model. For example, Fig. S1 (Supplementary Content) shows Langmuir and Freundlich isotherm models for the adsorption of C.I. Reactive Blue 19 onto hollow zein nanoparticles and C.I. Reactive Red 45 onto S. albus bacteria.[Xu et al., 2013, Kara et al., 2012]

## *5.2. Kinetic models*

Kinetic models are utilized to determine the mechanism of sorption process including the rate of adsorption, diffusion control, and mass transfer. Depending on the rate of adsorption, reaction kinetics could be first order and second order. Legergen proposed a first-order rate of reaction to describe the kinetic process of liquid-solid phase adsorption of oxalic acid and malonic acid onto charcoal [Ho, 2004], which is probably the first model to describe the rate of adsorption. The equation as:

——

Where $q_e$ and $q_t$ are the amounts of dye adsorbed (mg $g^{-1}$) at the equilibrium and at the time t (min), respectively, and $k_1$ is the pseudo-first order rate constant ($min^{-1}$). If the eq. 1 is integrated with the boundary conditions of $q_t = 0$ at t=0 and $q_t=q_t$ at t=t, then the equation can be written as [Ho, 1996]:

——

590 By rearranging equations 1 and 2, the pseudo-first-order equation can be expressed as

591591

592 ——

593 In 1995, a new kinetic model was proposed to describe the kinetics of divalent metal ion
594 uptake onto peat as the uptake followed the second order of reaction [Ho, 1996]. The
595 equation can be written as:

596 —_ — [12]

597 where $q_e$ and $q_t$ are the numbers of active sites occupied at the equilibrium and at the time t
598 (min), respectively, and $k_2$ is the pseudo-second-order rate constant (g $mg^{-1}$ $min^{-1}$). If the eq.
599 11 is integrated with the boundary conditions of $q_t = 0$ at t=0 and $q_t=q_t$ at t=t and rearranging,
600 the pseudo-second-order sorption rate can be written as:

— —— —

601 where $k_2$ is the pseudo-second-order rate constant ( g $mol^{-1}$ $min^{-1}$), and initial sorption rate (h)
602 is equal to $k_t q^2$ (( g $mol^{-1}$ $min^{-1}$). These two equations are mostly used describe the adsorption
603 of reactive dyes by various adsorbents. For example, it was reported that the adsorption of
604 C.I. Reactive Blue 19 onto L-arginine-functionalized $Fe_3O_4$ nanoparticles followed pseudo-
605 first-order and pseudo-second-order reaction rates as shown in Fig. S2 (Supplementary
606 Content) [Dalvand et al., 2016].

607607

## 608 6. Conclusions and future directions

609609

In this review, the research carried out using various ion-exchange resin-like adsorbents including modified clays, lignocellulosic biomasses, chitosan and its derivatives, microbial biomasses and magnetic particles investigated over the years for the treatment of dyehouse effluent containing reactive dyes have been critically discussed. The dye binding capacities of various types of adsorbents under different operating conditions are compared. The last decade has seen interest in developing biobased adsorbents as alternatives to activated carbon, especially lignocellulosic biomasses for the treatment of dyehouse effluent. However, the success achieved for the removal of reactive dyes is very limited because of their poor hydrodynamic properties, limited recycling and reusability, unpredictable adsorption behavior, and difficulty in regeneration compared to the activated carbon adsorbents. Some of the adsorbents, such as lignocellulosic adsorbents, investigated for the removal of reactive dyes showed poor dye binding capacity as the adsorbents and reactive dyes both are anionic. On the other hand, cationic chitosan showed excellent reactive dye-binding capacity. The literature survey shows that various cross-linked (such as epichlorohydrin and edetate) and quaternized chitosan provide the highest removal of reactive dyes. The synthesis methods of various ion-exchange adsorbents and chitosan derivatives are described. The dye binding capacity is affected by the molecular weight of the dyes and also by the functional groups of dyes. The adsorption of dyes into the adsorbents is affected by the adsorption time, pH, temperature, adsorbent dosage, the initial concentration of the dye in the effluent, and the type of adsorbent.

Almost all of these adsorbents have been investigated for the batch study using simulated reactive dye effluents but in industry, effluent treatment needs to be carried out in continuous mode. Therefore, further research will need to be carried out to determine their suitability for the continuous treatment of effluent. The adsorption treatments produce sludge, which needs

to be treated before their disposal. Therefore, appropriate treatment for the disposal of sludge also will need to be developed.

## Acknowledgement

The authors acknowledge the financial support received from the Ministry of Business, Innovation and Employment of New Zealand thorough Grant No. C10X0824.

## References

Abassi, M., Asl, N.R., 2009. Removal of hazardous reactive blue 19 dye from aqueous solution by agricultural waste. J. Iran. Chem. Res. 2, 221–230.

Adebayo, M.A., Prola, L.D.T., Lima, E.C., Puchana-Rosero, M.J., Cataluña, R., Saucier, C., Umpierres, C.S., Vaghetti, J.C.P., da Silva, L.G., Ruggiero, R., 2014. Adsorption of Procion Blue MX-R dye from aqueous solutions by lignin chemically modified with aluminium and manganese. J. Hazard. Mater. 268, 43–50.

Adsorptive removal of anionic dyes by chitosan-based magnetic microspheres with pH-responsive properties. J. Mol. Liquid. 256, 424–432.

Aguiar, J.E., Bezerra, B.T.C., Braga, B.M., Lima, P.D.S., Nogueira, R.E.F.Q., de Lucena, S.M.P., José da Silva Jr., I., 2013. Adsorption of anionic and cationic dyes from aqueous solution on non-calcined mg-al layered double hydroxide: experimental and theoretical study. Separat. Sci.Technol. (Philadelphia) 48, 2307–2316.

Akar, T., Sayin, F., Turkyilmaz, S., Tunali Akar, S., 2017. The feasibility of Thamnidium elegans cells for color removal from real wastewater. Process Safety Environ. Protect. 105, 316–325.

659 Akar, S. T., Akar, T., Çabuk, A., 2009. Decolorization of a textile dye, Reactive Red 198
660 (RR198), by Aspergillus parasiticus fungal biosorbent. Brazilian J. Chem. Eng. 26, 399–
661 405.
662 Aksu, Z., Cagatay, S.S., 2006. Investigation of biosorption of Gemazol Turquoise Blue-G
663 Reactive dye by dried Rhizopus arrhizus in batch and continuous systems. Sep. Purif.
664 Technol. 48, 24–35.
665 Aksu, Z., Tezer, S., 2000. Equilibrium and kinetic modelling of biosorption of Remazol
666 Black B by Rhizopus arrhizus in a batch system: effect of temperature. Process Biochem.
667 36, 431–9.
668 Aksu, Z., Tezer, S., 2005. Biosorption of reactive dyes on the green alga Chlorella vulgaris. J.
669 Process Biochem. 40, 1347–1361.
670 Aly, A.A., Mahmoud, S.A., El-Apasery, M.A., 2018. Decolorization of reactive dyes. Part I.
671 Eco-friendly approach of reactive dye effluents decolorization using cationized
672 sugarcane bagasse. Pigment Resin Technol. 47, 108–115.
673 Amin, M.T., Alazba, A.A., Shafiq, M., 2015. Adsorptive removal of reactive black 5 from
674 wastewater using bentonite clay: isotherms, kinetics and thermodynamics. Sustainability
675 7, 15302–15318.
676 Annadurai, G., Ling, L.Y., Lee, J.-F., 2008. Adsorption of reactive dye from an aqueous
677 solution by chitosan: Isotherm, kinetic and thermodynamic analysis. J. Hazard. Mater.
678 152, 337–346.
679 Argun, M.E., Guclu, D., Karatas, M., 2014. Adsorption of Reactive Blue 114 dye by using a
680 new adsorbent: Pomelo peel. J. Ind. Eng. Chem. 20, 1079–1084.
681 Ashori, A., Hamzeh, Y., Ziapour, A., 2014. Application of soybean stalk for the removal of
682 hazardous dyes from aqueous solutions. Polym. Eng. Sci. 54, 239–245.

683 Asouhidou, D.D., Triantafyllidis, K.S., Lazaridis, N.K., Matis, K.A., 2012. Adsorption of
684 reactive dyes from aqueous solutions by layered double hydroxides. J. Chem. Technol.
685 Biotechnol. 87, 575–582.
686 Auta, M., Hameed, B.H., 2014, Optimized and functionalized paper sludge activated with
687 potassium fluoride for single and binary adsorption of reactive dyes. J. Ind. Eng. Chem.
688 20, 830–840.

689 Aytar, P., Bozkurt, D., Erol, S., Özdemir, M., Çabuk, A., 2016. Increased removal of
690 Reactive Blue 72 and 13 acidic textile dyes by Penicillium ochrochloron fungus isolated
691 from acidic mine drainage. Desalin. Water Treat. 57, 19333–19343.
692 Bagchi, M., Ray, L., 2015. Adsorption behaviour of Reactive Blue 4, a triazine dye on dry
693 cells of Rhizopus oryzae in a batch system. Chem. Speciat. Bioavail. 27, 112–120.
694 Bayramoglu, G., Yilmaz, M., Arica, M.Y., 2010. Preparation and characterization of epoxy-
695 functionalized magnetic chitosan beads: Laccase immobilized for degradation of reactive
696 dyes. Bioprocess Biosys. Eng. 33, 439–448.
697 between the effects of nitrate, phosphate, boron and heavy metals on charophytes. New
698 Phytol. 189, 1051–1059.
699 Bharathi, K.S., Ramesh, S.T., 2013. Removal of dyes using agricultural waste as low-cost
700 adsorbents: a review. Appl. Water Sci. 3, 773–790.
701 Binupriya, A.R., Sathishkumar, M., Dhamodaran, K., Jayabalan, R., Swaminathan, K., Yun,
702 S.E., 2007. Liquid-phase separation of reactive dye by wood-rotting fungus: A
703 biotechnological approach. Biotechnol. J. 2, 1014–1025.
704 Bras, R., Ferra, I.A., Pinheiro, H.M., Goncalves, I.C. Batch tests for assessing decolorization
705 of azo dyes by methanogenic and mixed cultures. J. Biotechnol. 2001, 89, 155–162.

706 Cao, C., Xiao, L., Chen, C., Shi, X., Cao, Q., Gao, L., 2014. In situ preparation of magnetic
707 $Fe_3O_4$/chitosan nanoparticles via a novel reduction–precipitation method and their
708 application in adsorption of reactive azo dye. Powder Technol. 260, 90–97.
709 Cao, J.S., Lin, J.X., Fang, F., Zhang, M.T., Hu, Z.R., 2014. A new absorbent by modifying
710 walnut shell for the removal of anionic dye: kinetic and thermodynamic studies.
711 Bioresour. Technol. 163, 199–205.
712 Cardoso, N. F., Lima, E. C., Calvete, T., Pinto, I. S., Amavisca, C. V., Fernandes, T. H. M.,
713 Pinto, R.B., Alencar, W.S., 2011b. Application of aqai stalks as biosorbents for the
714 removal of the dyes Reactive Black 5 and Reactive Orange 16 from aqueous solution. J.
715 Chem. Eng. Data 56, 1857–1868.
716 Cardoso, N. F., Pinto, R., Lima, E. C., Pinto, I. S., 2011c. Removal of Remazol Black B
717 textile dye from aqueous solution by adsorption. Desalin. 269, 92–103.
718 Cardoso, N.F., Lima, E.C., Pinto, I.S., Amavisca, C.V., Royer, B., Pinto, R.B., Alencar, W.
719 S., Pereira, S.F.P., 2011a. Application of cupuassu shell as biosorbent for the removal of
720 textile dyes from aqueous solution. J. Environ. Manage. 92, 1237–1247.
721 Cardoso, N.F., Lima, E.C., Royer, B., Bach, M. V., Dotto, G.L., Pinto, L.A.A., Calvete, T.,
722 2012. Comparison of Spirulina platensis microalgae and commercial activated carbon as
723 adsorbents for the removal of Reactive Red 120 dye from aqueous effluents. J. Hazard.
724 Mater. 241–242, 146–153.
725 Çetin, D., Dönmez, G., 2006. Decolorization of reactive dyes by mixed cultures isolated from
726 textile effluent under anaerobic conditions. Enzyme Microb. Technol. 38, 926–930.
727 Chakraborty, S., Basu, J.K., De, S., Dasgupta, S., 2006. Adsorption of reactive dyes from a
728 textile effluent using sawdust as the adsorbent. Ind. Eng. Chem. Res. 45, 4732–4741.
729 Chang, J.-S., Chou, C., Chen, S.-Y., 2001. Decolorization of azo dyes with immobilized
730 Pseudomonas luteola. Process Biochem. 36, 757–763.

731 Chang, J.-S., Lin, Y.-C., 2000. Fed-batch bioreactor strategies for microbial decolorization of
732 azo dye using a Pseudomonas luteola strain. Biotechnol. Prog. 16, 979–985.
733 Chatterjee, S., Chatterjee, T., Woo, S.H., 2011. Influence of the polyethyleneimine grafting
734 on the adsorption capacity of chitosan beads for Reactive Black 5 from aqueous
735 solutions. Chem. Eng. J. 166, 168–175.
736 Chen, C.-Y., Chang, J.-C., Chen, A.-H., 2011. Competitive biosorption of azo dyes from
737 aqueous solution on the templated cross-linked-chitosan nanoparticles. J. Hazard. Mater.
738 185, 430-441.
739 Chinoune, K., Bentaleb, K., Bouberka, Z., Nadim, A., Maschke, U. Adsorption of reactive
740 dyes from aqueous solution by dirty bentonite. Appl. Clay Sci. 2016, 123, 64–75.
741 Chiou, M.-S., Ho, P.-Y., Li, H.-Y., 2004. Adsorption of anionic dyes in acid solutions using
742 chemically cross-linked chitosan beads. Dyes Pigm. 60, 69-84.
743 Chiou, M.-S., Kuo, W.-S., Li, H.-Y., 2003. Removal of reactive dye from wastewater by
744 adsorption using ECH cross-linked chitosan beads as medium. J. Environ. Sci. Health A,
745 38, 2621–2631.
746 Chiou, M.-S., Li, H.-Y., 2002. Equilibrium and kinetic modeling of adsorption of reactive
747 dye on cross-linked chitosan beads. J. Hazard. Mater. 93, 233–248.
748 Dalvand, A., Nabizadeh, R., Reza Ganjali, M., Khoobi, M., Nazmara, S., Hossein Mahvi, A.,
749 2016. Modelling of Reactive Blue 19 azo dye removal from colored textile wastewater
750 using L-arginine-functionalized $Fe_3O_4$ nanoparticles: Optimization, reusability, kinetic
751 and equilibrium studies. J. Magnet. Magnetic Mater. 404, 179–189.
752 de Jesus, C. P. C., Antunes, M. L. P., da Conceição, F. T., Navarro, G. R. B., Moruzzi, R. B.,
753 2015. Removal of reactive dye from aqueous solution using thermally treated red mud.
754 Desalin. Water Treat. 55, 1040–1047.

de Souza, K.C., Antunes, M.L.P., Couperthwaite, S.J., da Conceição, F.T., de Barros, T.R., Frost, R., 2013. Adsorption of reactive dye on seawater-neutralized bauxite refinery residue. J. Colloid Interf. Sci. 396, 210–214.

Debrassi, A., Baccarin, T., Demarchi, C. A., Nedelko, N., Ślawska-Waniewska, A., Dluzewski, P., Bilska, M., Rodrigues, C.A., 2012. Adsorption of Remazol Red 198 onto magnetic N-lauryl chitosan particles: Equilibrium, kinetics, reuse and factorial design. Environ. Sci. Pollution Res. 19, 1594–1604.

Demarchi, C. A., Debrassi, A., de Campos Buzzi, F., Nedelko, N., Ślawska-Waniewska, A., Dłuzewski, P., Dal Magro, J., Scapinello, J., Rodrigues, C.A., 2015. Adsorption of the dye Remazol Red 198 (RR198) by O-carboxymethylchitosan-N-lauryl/γ-$Fe_2O_3$ magnetic nanoparticles. Arab. J. Chem. 8. DOI: 10.1016/j.arabjc.2015.08.028

Dhanapal, V., Subramanian, K., 2014. Recycling of textile dye using double network polymer from sodium alginate and superabsorbent polymer. Carbohyd. Polym. 108, 65–74.

Dharajiya, D., Shah, M., Bajpai, B., 2016. Decolorization of simulated textile effluent by Phanerochaete chrysosporium and Aspergillus fumigatus A23. Nature Environ. Pollut. Technol. 15, 825–832.

Dubinin, M.M., Radushkevich, L.V., 1947. The equation of the characteristic curve of the activated charcoal. Proc. Acad. Sci. USSR Phys. Chem. Sect. 55, 331–337.

Duman, O., Tunç, S., Bozoğlan, B. K., Polat, T.G., 2016. Removal of triphenylmethane and reactive azo dyes from aqueous solution by magnetic carbon nanotube-κ-carrageenan-$Fe_3O_4$ nanocomposite. J. Alloys Comp. 687, 370–383.

El-Naggar, M.E., Radwan, E.K., El-Wakeel, S.T., Kafafy, H., Gad-Allah, T.A., El-Kalliny, A.S., Shaheen, T.I., 2018. Synthesis, characterization and adsorption properties of

779 microcrystalline cellulose-based nanogel for dyes and heavy metals removal. Int. J.
780 Biologic. Macromol. 113, 248-258.
781 Elwakeel, K.Z., 2009. Removal of Reactive Black 5 from aqueous solutions using magnetic
782 chitosan resins. J. Hazard. Mater. 167, 383–392.
783 Errais, E., Duplaya, J., Elhabiri, M., Khodjac, M., Ocampod, R., Baltenweck-Guyote, R.,
784 Darragi, F., 2012. Anionic RR120 dye adsorption onto raw clay: surface properties and
785 adsorption mechanism. Colloids Surf. A, 403, 69–78
786 Ferrero, F., 2007. Dye removal by low cost adsorbents: hazelnut shells in comparison with
787 wood sawdust. J. Hazard. Mater. 142, 144–52.
788 Fettouche, S., Tahiri, M., Madhouni, R., Cherkaoui, O., 2015. Removal of reactive dyes from
789 aqueous solution by adsorption onto Alfa fibers powder. J. Mater. Environ. Sci. 6, 129–
790 137.
791 Figueiredo, S.A., Boaventura, R.A., Loureiro, J.M., 2000. Color removal with natural
792 adsorbents: Modelling, simulation and experimental. Separat. Purific. Technol. 20, 129–
793 141.
794 Filipkowska, U. Adsorption and desorption of reactive dyes onto chitin and chitosan flakes
795 and beads. Adsorp. Sci. Technol. 2006, 24, 781–795.
796 Fontana, J.D., Baldo, G.R., Grzybowski, A., Tiboni, M., Scremin, L.B., Koop, H.S., Santana,
797 M.J., Lião, L.M., Döhler, L., 2016. Textile cotton dust waste: partial diethylamino-
798 ethylation and its application to the sorption/removal of the model residual textile dye
799 Reactive Red 239. Polym. Bull. 73, 3401–3420.
800 Freundlich, H.M.F. Over the adsorption in solution. J. Phys. Chem. 1906, 57, 385–471.
801 Gao, J., Si, C., He, Y., 2015. Application of soybean residue (okara) as a low-cost adsorbent
802 for reactive dye removal from aqueous solution. Desalin. Water Treat. 53, 2266–2277.

Ghaneian, M.T., Jamshidi, B., Dehvari, M., Amrollahi, M., 2015. Pomegranate seed powder as a new biosorbent of reactive red 198 dye from aqueous solutions: Adsorption equilibrium and kinetic studies. Res. Chem. Intermed. 41, 3223–3234.

Gingell, R., Walker, R., 1971. Mechanisms of azo reduction by Streptococcus faecalis. II. The role of soluble flavins. Xenobiotica 1, 231–9.

Guendouz, S., Khellaf, N., Djelal, H., Ouchefoun, M., 2016. Simultaneous biosorption of the two synthetic dyes, Direct Red 89 and Reactive Green 12 using nonliving macrophyte L. gibba L. Desalin. Water Treat. 57, 4624–4632.

Gül, Ü. D., Dönmez, G., 2013. Application of mixed fungal biomass for effective reactive dye removal from textile effluents. Desalin. Water Treat. 51, 3597–3603.

Gunay, A., Arslankaya, E., Tosun, I., 2007. Lead removal from aqueous solution by natural and pre-treated clinoptilolite: adsorption equilibrium and kinetics. J. Hazard. Mater. 146, 362–371.

Hassan, M.M., 2014. Enhanced antistatic and mechanical properties of corona plasma-treated wool fabrics treated with 2,3-epoxypropyltrimethylammonium chloride. Ind. Eng. Chem. Res. 53, 10954–10964.

Hassan, M.M., 2015. Binding of a quaternary ammonium polymer-grafted-chitosan onto a chemically modified wool fabric surface: Assessment of mechanical, antibacterial and antifungal properties. RSC Adv. 5, 35497–35505.

Ho, Y.S., 2004. Citation review of Lagergren kinetic rate equation on adsorption reactions. Scientometrics 59, 171–177.

Ho, Y.S., Wase, D.A.J., Forster, C.F., 1996. Removal of lead ions from aqueous solution using sphagnum moss peat as adsorbent. Water SA 22, 219–224.

826 Honorio, J.F., Veit, M.T., Da Cunha Gonçalves, G., De Campos, E.A., Fagundes-Klen, M.R.,
827 2016. Adsorption of reactive blue BF-5G dye by soybean hulls: Kinetics, equilibrium
828 and influencing factors. Water Sci. Technol. 73, 1166–1174.
829 Hu, T.L., 1996. Removal of reactive dyes from aqueous solution by different bacterial
830 genera. Water Sci. Technol. 34, 89–95.
831 Ignat, M.-E., Dulman, V., Onofrei, T., 2012. Reactive Red 3 and Direct Brown 95 dyes
832 adsorption onto chitosan. Cellulose Chem. Technol. 46, 357–367.
833 Iscen, C.F., Kiran, I., Ilhan, S., 2007. Biosorption of Reactive Black 5 dye by Penicillium
834 restrictum: The kinetic study. J. Hazard. Mater. 143, 335–340.
835 Jafari, A.J., Kakavandi, B., Kalantary, R.R., Gharibi, H., Asadi, A., Azari, A., Babaei, A.A.,
836 Takdastan, A., 2016. Application of mesoporous magnetic carbon composite for reactive
837 dyes removal: Process optimization using response surface methodology. Korean J.
838 Chem. Eng. 33, 2878–2890.
839 Janaki, V., Vijayaraghavan, K., Oh, B.-T., Lee, K.-J., Muthuchelian, K., Ramasamy, A.K.,
840 Kamala-Kannan, S., 2012. Starch/polyaniline nanocomposite for enhanced removal of
841 reactive dyes from synthetic effluent. Carbohyd. Polym. 90, 1437–1444.
842 Jiang, X., Sun, Y., Liu, L., Wang, S., Tian, X., 2014. Adsorption of C.I. Reactive Blue 19
843 from aqueous solutions by porous particles of the grafted chitosan. Chem. Eng. J. 235,
844 151–157.
845 Jóźwiak, T., Filipkowska, U., Szymczyk, P., Kuczajowska-Zadrożna, M., Mielcarek, A.,
846 2015. Application of chitosan ionically cross-linked with sodium edetate for reactive
847 dyes removal from aqueous solutions. Prog. Chem. Applicat. Chitin Derivat. 20, 82–96.
848 Kadam, A.A., Lee, D.S., 2015. Glutaraldehyde cross-linked magnetic chitosan
849 nanocomposites: Reduction precipitation synthesis, characterization, and application for
850 removal of hazardous textile dyes. Bioresour. Technol. 193, 563–567.

851 Kalkan, E., Nadaroğlu, H., Celebi, N., Tozsin, G., 2014. Removal of textile dye Reactive
852 Black 5 from aqueous solution by adsorption on laccase-modified silica fume. Desalin.
853 Water Treat. 52, 6122–6134.

854 Kannusamy, P., Sivalingam, T., 2013. Synthesis of porous chitosan-polyaniline/ZnO hybrid
855 composite and application for removal of reactive orange 16 dye. Colloid. Surf. B:
856 Biointerf. 108, 229–238.

857 Kara, I., Akar, S. T., Akar, T., Ozcan, A., 2012. Dithiocarbamated Symphoricarpus albus as a
858 potential biosorbent for a reactive dye. Chem. Eng. J. 211–212, 442–452.

859 Karcher, S., Kornmuller, A., Jekel, M., 2002. Anion exchange resins for removal of reactive
860 dyes from textile wastewaters. Water Res. 36, 4717–4724.

861 Karim, M.E., Dhar, K., Hossain, M.T., 2017. Co-metabolic decolorization of a textile reactive
862 dye by Aspergillus fumigatus. Int. J. Environ. Sci. Technol. 14, 177–186.

863 Khoshhesab, Z. M., Gonbadi, K., Rezaei Behbehani, G., 2015. Removal of reactive black 8
864 dye from aqueous solutions using zinc oxide nanoparticles: Investigation of adsorption
865 parameters. Desalin. Water Treat. 56, 1558–1565.

866 Kim, S., Won, S.W., Cho, C.-W., Yun, Y.-S., 2016. Valorization of Escherichia coli waste
867 biomass as a biosorbent for removing reactive dyes from aqueous solutions. Desalin.
868 Water Treat. 57, 20084–20090.

869 Kim, S.-Y., 2007. Improvement of the decolorization of azo dye by anaerobic sludge
870 bioaugmented with Desulfovibrio desulfuricans. Biotechnol. Bioproc. Eng. 12, 222–227.

871 Kim, T.-Y., Park, S.-S., Cho, S.-Y., 2012. Adsorption characteristics of Reactive Black5 onto
872 chitosan beads cross-linked with epichlorohydrin. J. Ind. Eng. Chem. 18, 1458–1464.

873 Kumari K., Abraham T.E., 2007. Biosorption of anionic textile dyes by nonviable biomass of
874 fungi and yeast. Bioresour. Technol. 98, 1704–10.

875 Kyzas, G.Z., Fu, J., Matis, K.A., 2013. The Change from past to future for adsorbent
876 materials in treatment of dyeing wastewaters. Materials 6, 5131–5158.
877 Kyzas, G.Z., Lazaridis, N.K., 2009. Reactive and basic dyes removal by sorption onto
878 chitosan derivatives. J. Colloid Interf. Sci. 331, 32–39.
879 Lagergren, S., 1898. About the theory of so-called adsorption of soluble substances. Kungliga
880 Svenska Vetenskapsakademiens, Handlingar 24, 1–39.
881 Lambert, S J., Davy, A.J., 2011. Water quality as a threat to aquatic plants: discriminating
882 Langmuir, I., 1916. The constitution and fundamental properties of solids and liquids. J. Am.
883 Chem. Soc. 38, 2221–2295.
884 Li, Z., Cao, M., Zhang, W., Liu, L., Wang, J., Ge, W., Yuan, Y., Yue, T., Li, R., Yu, W.W.,
885 2014. Affinity adsorption of lysozyme with Reactive Red 120 modified magnetic
886 chitosan microspheres. Food Chem. 145, 749–755.
887 Lima, E. C., Royer, B., Vaghetti, J. C. P., Simon, N. M., da Cunha, B. M., Pavan, F. A.,
888 Benvenutti, E.V., Veses, R.C., Airoldi, C., 2008. Application of Brazilian-pine fruit coat
889 as a biosorbent to removal of reactive red 194 textile dye from aqueous solution, Kinetics
890 and equilibrium study. J. Hazard. Mater. 155, 536–550.
891 Low, K.S., Lee, C.K., 1997. Quaternized rice husk as sorbent for reactive dyes. Bioresour.
892 Technol. 61, 121–125.
893 Low, K.-S., Lee, C.-K., Tan, B.-F., 2000. Quaternized wood as sorbent for reactive dyes.
894 Appl. Biochem. Biotechnol. A: Enzyme Eng. Biotechnol. 87, 233–245.
895 Ma, Q., Wang, L., 2015. Adsorption of Reactive blue 21 onto functionalized cellulose under
896 ultrasonic pretreatment: Kinetic and equilibrium study. J. Taiwan Inst. Chem. Eng. 50,
897 229–235.

898 Meehan, C., Bjourson, A.J., McMullan, G., 2001. *Paenibacillus azoreducens sp. no*v., a
899 synthetic azo dye decolorizing bacterium from industrial wastewater. Int. J. System.
900 Evolution. Microbiol. 51, 1681–1685.
901 Mona, S., Kaushik, A., Kaushik, C.P., 2011. Waste biomass of Nostoc linckia as adsorbent of
902 crystal violet dye: Optimization based on statistical model. Int. Biodeterior. Biodegrad.
903 65, 513–521.
904 Morais, L.C., Freitas, O.M., Goncalves, E.P., Vasconcelos, L.T., Gonzalez Beca, C.G., 1999.
905 Reactive dyes removal from wastewaters by adsorption on Eucalyptus bark: variables
906 that define the process. Water Res. 33, 979–988.
907 Nadafi, K., Vosoughi, M., Asadi, A., Borna, M. O., Shirmardi, M., 2014. Reactive Red 120
908 dye removal from aqueous solution by adsorption on nano-alumina. J. Water Chem.
909 Technol. 36, 125–133.
910 Ncibi, M. C., Mahjoub, B., Seffen, M. Adsorptive removal of textile reactive dye using
911 Posidonia oceanic (L) fibrous biomass. Int. J. Environ. Sci. Technol. 2007, 4, 433–440.
912 Nga, N.K., Chinh, H.D., Hong, P.T.T., Huy, T.Q., 2017. Facile preparation of chitosan films
913 for high-performance removal of Reactive Blue 19 dye from aqueous solution. J. Polym.
914 Environ. 25, 146–155.
915 Ovando-Medina, V. M., Vizcaíno-Mercado, J., González-Ortega, O., De La Garza, J. A. R.,
916 Martínez-Gutiérrez, H., 2015. Synthesis of α-cellulose/polypyrrole composite for the
917 removal of reactive red dye from aqueous solution: Kinetics and equilibrium modeling.
918 Polym. Compos. 36, 312–321.
919 Oxspring, D.A., McMullan, G., Smyth, W.F., Marchant, R., 1996. Decolorization and
920 metabolism of the reactive textile dye, Remazol Black B, by an immobilized microbial
921 consortium. Biotechnol. Lett. 18, 527–30.

922 Pearce, C.I., Lloyd, J.R., Guthrie, J.T., 2003. The removal of color from textile wastewater
923 using whole bacterial cells: A review. Dyes Pigment. 58, 179–196.
924 Plumb, J.J., Bell, J., Stuckey, D.C., 2001. Microbial populations associated with treatment of
925 an industrial dye effluent in an anaerobic baffled reactor. Appl. Environ. Microbiol. 67,
926 3226–35.
927 Rahman, A., Urabe, T., Kishimoto, N., 2013. Color removal of Prion reactive dyes by clay
928 adsorbents. Procedia Environ. Sci. 17, 270–278.
929 Ratnamala, G. M., Deshannavar, U. B., Munyal, S., Tashildar, K., Patil S., Shinde, A.,
930 2016. Adsorption of reactive blue dye from aqueous solutions using sawdust as
931 adsorbent: Optimization, kinetic, and equilibrium studies. Arabian J. Sci. Eng. 41, 333–
932 344.
933 Reddy, M.C.S, Nirmala, V., Ashwini, C., 2017. Bengal Gram Seed Husk as an adsorbent for
934 the removal of dye from aqueous solutions – Batch studies. Arab. J. Chem. 10, 2554–
935 S2566.
936 Redlich, O., Peterson, D.L., 1959. A useful adsorption isotherm. J. Phys. Chem. 63, 1024–
937 1026.
938 Robinson, T., McMullan, G., Marchant, R., Nigam, P., 2001. Remediation of dyes in textile
939 effluent: A critical review on current treatment technologies with a proposed alternative.
940 Bioresour. Technol. 77, 247–55.
941 Rosa, S., Laranjeira, M.C.M., Riela, H.G., Fávere, V.T., 2008. Cross-linked quaternary
942 chitosan as an adsorbent for the removal of the reactive dye from aqueous solutions. J.
943 Hazard. Mater. 155, 253–260.
944 Saeed, M., Nadeem, R., Yousaf, M., 2015. Removal of industrial pollutant (Reactive Orange
945 122 dye) using environment-friendly sorbent Trapa bispinosa's peel and fruit. Int. J.
946 Environ. Sci. Technol. 12, 1223–1234.

947 Samarghandi, M.R., Hadi, M., Moayedi, S., Askari, F.B., 2009. Two-parameter isotherms of
948 methyl orange sorption by pinecone derived activated carbon. Iranian J. Environ. Health
949 Sci. Eng. 6, 285–294.
950 San Keskin, N.O., Celebioglu, A., Sarioglu, O.F., Ozkan, A.D., Uyar, T., Tekinay, T., 2015.
951 Removal of a reactive dye and hexavalent chromium by a reusable bacteria attached
952 electrospun nanofibrous web. RSC Adv. 5, 86867–86874.
953 Shuang, C., Li, P., Li, A., Zhou, Q., Zhang, M., Zhou, Y., 2012. Quaternized magnetic
954 microspheres for the efficient removal of reactive dyes. Water Res. 46, 4417–4426.
955 Sinha, A., Osborne, W.J., 2016. Biodegradation of reactive green dye (RGD) by indigenous
956 fungal strain VITAF-1. Int. Biodeterior. Biodegrad. 114, 176–183.
957 Sips, R., 1948. Combined form of Langmuir and Freundlich equations. J. Chem. Phys. 16,
958 490–495.
959 Song, K., Xu, H., Xu, L., Xie, K., Yang, Y., 2017. Cellulose nanocrystal-reinforced keratin
960 bioadsorbent for effective removal of dyes from aqueous solution. Bioresour. Technol.
961 232, 254–262.
962 Subramani, S.E., Thinakaran, N., 2017. Isotherm, kinetic and thermodynamic studies on the
963 adsorption behavior of textile dyes onto chitosan. Process Safety Environ. Protec. 106,
964 1–10.
965 Sumari, S. M., Hamzah, Z., Kantasamy, N., 2016. Adsorption of anionic dyes from aqueous
966 solutions by calcined and uncalcined Mg/Al layered double hydroxide. Malaysian J.
967 Anal. Sci. 20, 777–792.
968 Sun, D., Zhang, Z., Wang, M., Wu, Y., 2013. Adsorption of reactive dyes on activated carbon
969 developed from Enteromorpha prolifera. Am. J. Analyt. Chem. 4, 17–26.
970 Tanyildizi, M.S., 2011. Modeling of adsorption isotherms and kinetics of reactive dye from
971 aqueous solution by peanut hull. Chem. Eng. J. 168, 1234–1240.

Toth, J., 1971. State equations of the solid-gas interface layer. Acta Chem. Acad. Hung. 69, 311–317.

Vakili, M., Rafatullah, M., Salamatinia, B., Ibrahim, M.H., Abdullah, A.Z., 2015. Elimination of reactive blue 4 from aqueous solutions using 3-aminopropyl triethoxysilane modified chitosan beads. Carbohyd. Polym. 132, 89–96.

Venkatesha, T.G., Viswanatha, R., Arthoba Nayaka, Y., Chethana, B.K., 2012. Kinetics and thermodynamics of reactive and vat dyes adsorption on MgO nanoparticles. Chem. Eng. J. 198–199, 1–10.

Vijayaraghavan, K., Padmesh, T.V.N., Palanivelu, K., Velan, M., 2006. Biosorption of nickel(II) ions onto Sargassum wightii: application of two-parameter and three parameter isotherm models. J. Hazard. Mater. B133, 304–308.

Vijayaraghavan, K., Yun, Y.S., 2007. Utilization of fermentation waste (Corynebacterium glutamicum) for biosorption of Reactive Black 5 from aqueous solution. J. Hazard. Mater. 141, 45–52.

Wang, P., Ma, Q., Hu, D., Wang, L., 2015. Removal of Reactive Blue 21 onto magnetic chitosan microparticles functionalized with polyamidoamine dendrimers. React. Function. Polym. 91–92, 43–50.

Wang, Q., Luan, Z., Wei, N., Li, J., Liu, C., 2009. The color removal of dye wastewater by magnesium chloride/red mud (MRM) from aqueous solution. J. Hazard. Mater. 170, 690–698.

Won, S.W., Kim, H.J., Choi, S.H., Chung, B.W., Kim, K.J., Yun, Y.S., 2006. Performance, kinetics and equilibrium in biosorption of anionic dye Reactive Black 5 by the waste biomass of Corynebacterium glutamicum as a low-cost biosorbent. Chem. Eng. J. 121, 37–43.

Won, S.W., Yun, Y.S., 2008. Biosorptive removal of Reactive Yellow 2 using waste biomass from lysine fermentation process. Dyes Pigm. 76, 502–507.

Wong, S.Y., Tan, Y.P., Abdullah, A.H., Ong, S.T., 2009. The removal of basic and reactive dyes using quaternized sugarcane bagasse. J. Phys. Sci. 20, 59–74.

Xie, X., Li, X., Luo, H., Lu, H., Chen, F., Li, W., 2016. The adsorption of reactive blue 19 dye onto cucurbit[8]uril and cucurbit[6]uril: An experimental and theoretical study. J. Phys. Chem. B 120, 4131–4142.

Xu, B., Zheng, H., Zhou, H., Wang, Y., Luo, K., Zhao, C., Peng, Y., Zheng, X., 2018.

Xu, H., Zhang, Y., Jiang, Q., Reddy, N., Yang, Y., 2013. Biodegradable hollow zein nanoparticles for removal of reactive dyes from wastewater. J. Environ. Manag. 125, 33-40.

Xue, A., Zhou, S., Zhao, Y., Lu, X., Han, P., 2010. Adsorption of reactive dyes from aqueous solution by silylated palygorskite. Appl. Clay Sci. 48, 638–640.

Yagub, M.T., Sen, T.K., Afroze, S., Ang, H.M., 2014. Dye and its removal from aqueous solution by adsorption: A review. Adv. Colloids Interf. Sci. 209, 172–184.

## Graphical abstract

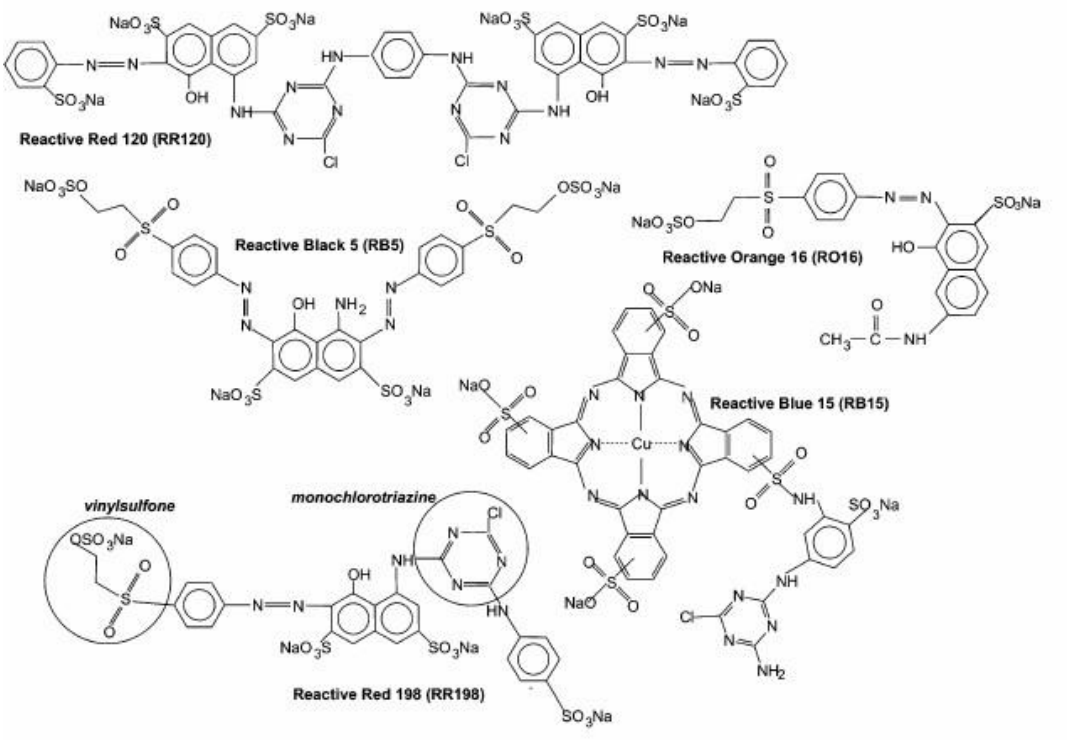


**Fig. 1.** Chemical structure of some common reactive dyes used for the decolourisation studies (Karcher et al., 2002).

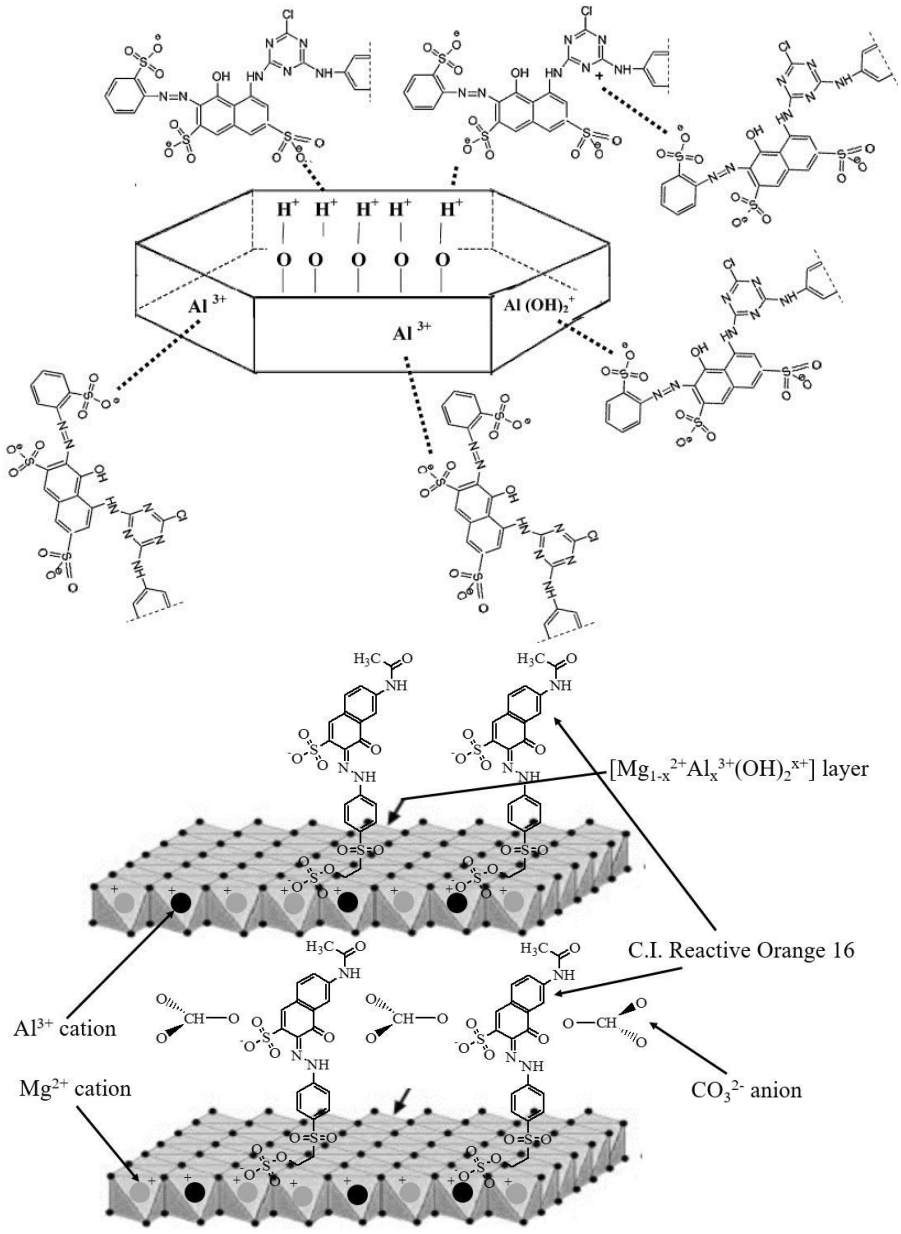


**Fig. 2.** Adsorption mechanisms of C.I. Reactive Red 120 and C.I. Reactive Orange 16 dye molecules onto kaolinite clay sheets (top) and Mg/Al layered double hydroxides (bottom) respectively (Khoshhesab et al., 2015).

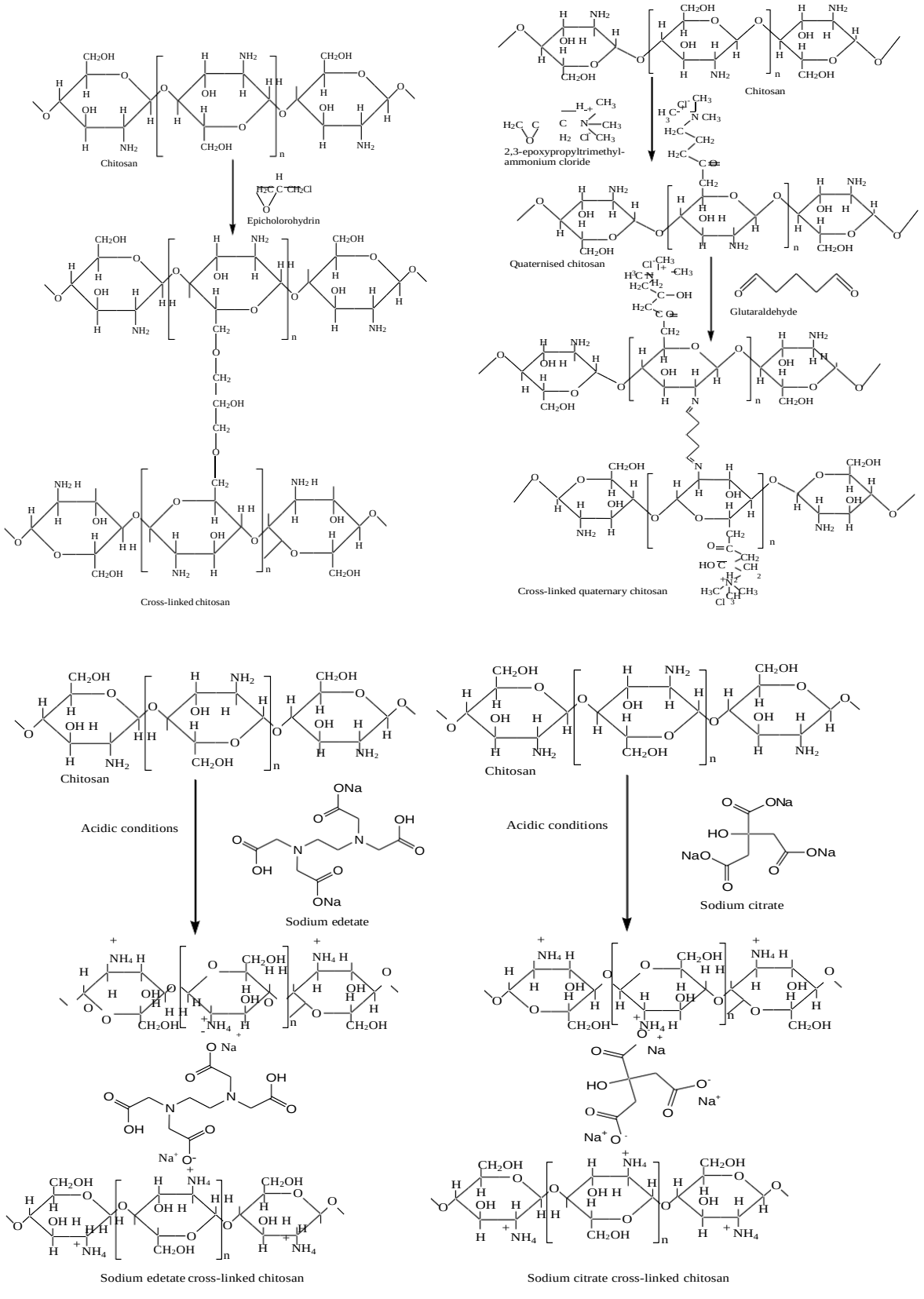


**Fig. 3.** Formation mechanism of chitosan adsorbents by ionic cross-linking (top) as well as by covalent bond forming cross-linking.

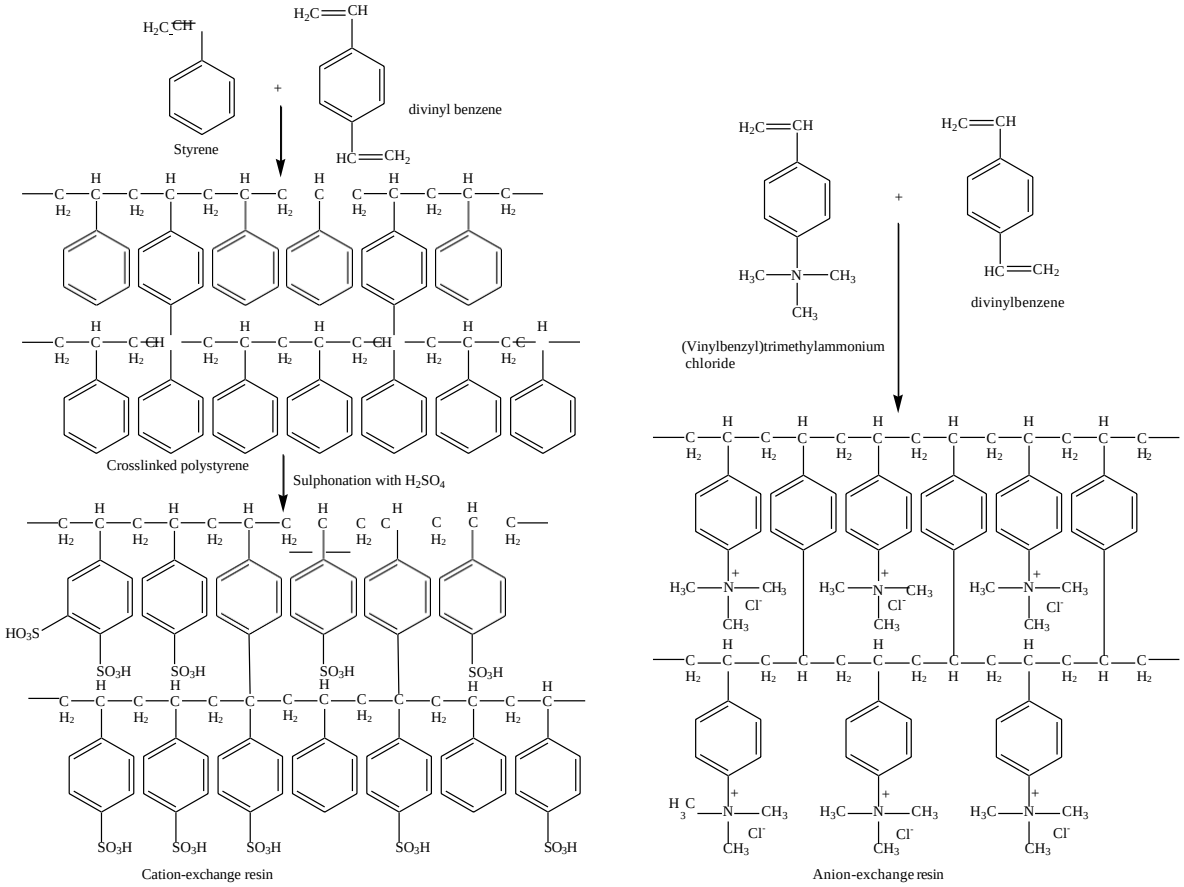


**Fig. 4.** Synthesis of cation-exchange and anion-exchange resins from styrene and (vinylbenzyl)ammonium chloride respectively by free-radical polymerisation method.

— — — — — —

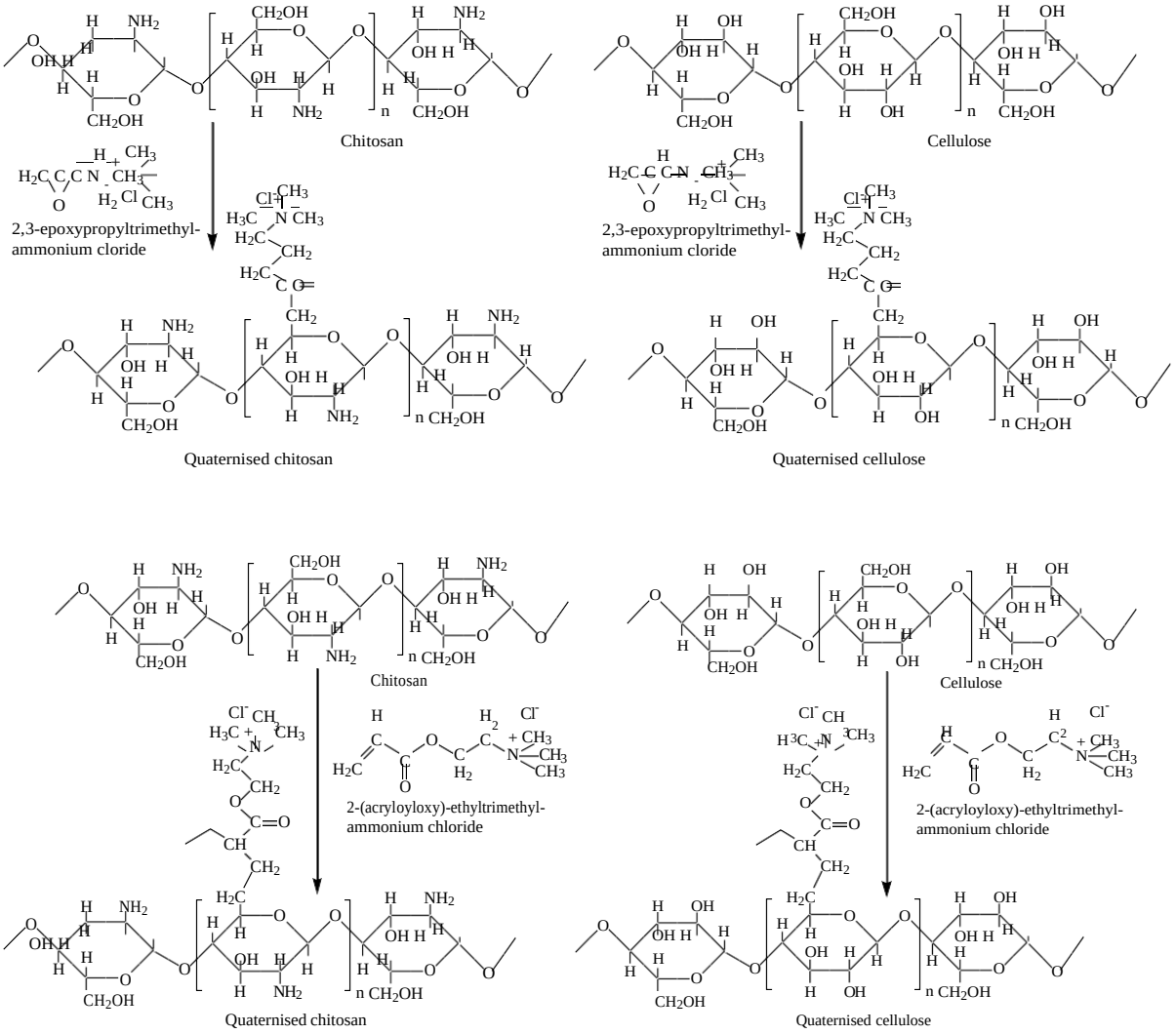


**Fig. 5.** Formation of quaternised chitosan and cellulose adsorbents by chemical modification with an epoxy group-containing quaternary ammonium compound (top) and by graft-copolymerisation with 2-(acryloyloxy)ethyltrimethylammonium chloride (Hassan, 2015; Hassan, 2014).

**Table 1**

Reactive dye binding capacity and performance of various types of ion-exchange resin adsorbents

| Ion-exchange resins | Dye type | Treatment methods | Operating conditions | | | | | | Dye binding capacity (mg $g^{-1}$) | Ref. |
|---|---|---|---|---|---|---|---|---|---|---|
| | | | Temperature of treatment (°C) | Optimum pH | Dosage of sorbent (g $l^{-1}$) | Agitation speed (rpm) | Dye conc. (mg $l^{-1}$) | Contact time (min) | | |
| Bayer anion exchange resin ( S6328a) having quarternary amine and trymethylamine groups | Reactive Black 5<br>Reactive Red 198 | Batch | 20–25 | 2 | 2 | n/a | 2000 | 4320 | 694.25<br>590.50 | [Karcher et al., 2002] |
| Bayer anion exchange resin (MP62) having tertiary amine groups | Reactive Black 5<br>Reactive Red 198 | Batch | 20–25 | 2 | 2 | n/a | 2000 | 4320 | 1190.14<br>n/a | [Karcher et al., 2002] |
| SR Amberlite IRC-718 anion exchange resin | Reactive Blue 2<br>Reactive Orange 16<br>Reactive Yellow 2 | Batch | 23±2 | n/a | 5 | 150 | 500 | 240 | 1.26<br>3.86<br>3.66 | [Low and Lee, 1997] |
| Quaternised rice husks | Reactive Blue 2<br>Reactive Orange 16<br>Reactive Yellow 2 | Batch | 23±2 | n/a | 5 | 150 | 500 | 240 | 4.90<br>4.40<br>5.00 | [Low and Lee, 1997] |
| Poly(AA-NIPAAm-TMPTA) crosslinked with sodium alginate | C.I. Reactive Blue 4 | Column | 30 | 6 | 100 ml dye 10 $g^{-1}$ adsorbent | - | 5000 | 30 | 446 | [Dhanapal, 2014] |
| Partial diethylamino-ethylated cotton dust waste | C.I. Reactive Red 239 | Batch | 25 | 6.6 | 5 | 160 | 500 | 1440 | 86.96 | [Fontana et al., 2016] |
| Quaternised wood | Reactive Blue 2 | Batch | 28±2 | 11 | 5 | 150 | 2000 | 360 | 250.00 | [Low et al., 2000] |
| Quaternised flax cellulose with ultrasound | Reactive Blue 21 | Batch | 30 | 9 | 0.31 | 120 | 200 | 180 | 543.00 | [Ma and Wang, 2015] |
| Cucurbit[8]uril<br>Cucurbit[6]uril | C.I. Reactive Blue 19 | Batch | 25<br>24 | 7 | 0.3 | n/a | 300 | 720 | 714.29<br>100.5 | [Xie et al., 2016] |

| | | | | | | | | | | |
|---|---|---|---|---|---|---|---|---|---|---|
| Quaternised sugarcane bagasse | C.I. Reactive Orange 16 | Batch | 25 | 3 | 5 | 150 | 100 | 480 | 22.73 | [Wong et al., 2009] |
| Ethylenediamine functionalised activated paper sludge | Reactive Blue 19 | Batch | 30 | 2 | 0.4 | n/a | 200 | 1440 | 689.97 | [Auta and Hameed, 2014] |
| Potassium fluoride activated paper sludge | Reactive Orange 16 | | | | | | | | 696.23 | |
| Cellulose nanocrystal-reinforced keratin | Reactive Black 5 | Batch | 25 | 2 | 2 | n/a | 200 | 180 | 1250 | [Song et al., 2017] |
| Starch/polyaniline nanocomposite | Reactive Black 5 | Batch | 25 | 3 | 0.6 | 150 | n/a | 70 | 811.3 | [Janaki et al., 2012] |
| | Reactive Violet 4 | | | | | | | | 578.39 | |
| Polypyrrole-modified-α-cellulose | Reactive Red 120 | Batch | 25 | 2 | 3.33 | n/a | 1000 | 8640 | 96.1 | [Ovando-Medina et al, 2015] |
| Hollow zein nanoparticles | C.I. Reactive Blue 19 | Batch | 25 | 2 | 1 | n/a | 75–2260.5 | 1440 | 1016.00 | [Xu et al., 2013] |
| Lignin chemically modified with aluminium | Reactive Blue 4 | Batch | 25 | 2 | 2.5 | n/a | 340 | 480 | 73.52 | [Adebayo et al., 2014] |
| Lignin chemically modified with manganese | | | | | | | | | 55.16 | |
| Cationic polyelectrolyte polyepicholorohydrin-dimethylamine modified bentonite | Reactive Blue 4 | Batch | 30 | 2 | 2 | n/a | 150 | 120 | 63.19 | [Chen et al., 2011] |
| | Reactive yellow 18 | | | | | | | | 110..64 | |

**Table 2**

Reactive dye removal performance of lignocellulosic biomasses.

| Ion-exchange resins | Dye type | Treatment methods | Operating conditions | | | | | | Dye binding capacity (mg $g^{-1}$) | Ref. |
|---|---|---|---|---|---|---|---|---|---|---|
| | | | Temperature of treatment (°C) | Optimum pH | Dosage of sorbent (g $l^{-1}$) | Agitation speed (rpm) | Dye conc. (mg $l^{-1}$) | Contact time (min) | | |
| Trapa bispinosa's peel | C.I. Reactive Orange 122 | Batch | n/a | 1 | 2 | 100 | 350 | 120 | 29.79 | [Saeed et al., 2015] |
| Trapa bispinosa's fruit | C.I. Reactive Orange 122 | Batch | n/a | 1 | 2 | 100 | 350 | 120 | 29.51 | [Saeed et al., 2015] |
| Grape fruit peel | C.I. Reactive Blue 19 | Batch | n/a | 3 | 3.33 | 180 | 50 | 45 | 12.53 | [Abassi and Asl, 2009] |
| Alfa fibres powder | C.I. Reactive Red 23 | Batch | 22 | 2 | 30 | 150 | 100 | 90 | 34.13 | [Fettouche et al., 2015] |
| | C.I. Reactive Blue 19 | | | | | | | | 11.33 | |
| soybean residue | C.I. Reactive Blue 19 | Batch | 50 | 2 | x | x | x | x | 402.58 | [Gao et al., 2015] |
| soybean stalk | C.I. Reactive Black 5 | Batch | 20±1 | 2 | 15 | 100 | 150 | 720 | 9.90 | [Ashori et al., 2014] |
| Soybean hull | C.I. Reactive Blue 25 | Batch | 25 | 2 | 6 | 100 | 400 | 1440 | 57.47 | [Honorio et al., 2016] |
| Eucalyptus bark | C.I. Reactive Blue 19 | Batch | 18 | 2.5 | 2 | 70 | 0.5 | 4320 | 90 | [Morais et al., 1999] |
| Acid treated Brazilian pine fruit coat, | C.I. Reactive Red 194 | Batch | 25 | 2 | 1-25 | n/a | 500 | 4320 | 51.9 | [Lima et al., 2008] |
| Modified walnut shell | Reactive Red | Batch | 40 | 2.5 | 6 | 180 | 20-1000 | 300 | 568.2 | [Cao et al., 2014] |
| Cupuassu shell | C.I. Reactive Black 5 | Batch | 25 | 2 | 10 | n/a | 250 | 2880 | 22.9 | [Cardoso et al., 2011a] |
| *P. oceanica* leaf sheaths | C.I. Reactive Red 228 | Batch | 60 | 5 | 20 | 100 | 100 | 2880 | 3.50 | [Ncibi et al., 2007] |
| Aqai palm stalk powder | C.I. Reactive | Batch | 25 | 2 | 1-10 | n/a | 300 | 2880 | 52.3 | [Cardoso et al., |

| | | | | | | | | | | |
|---|---|---|---|---|---|---|---|---|---|---|
| | Black 5 | | | | | | | | | 2011b] |
| | C.I. Reactive Orange 16 | | | | | | | | 61.3 | |
| Acid-treated Aqai palm stalk powder | C.I. Reactive Black 5 | | | | | | | | 72.3 | |
| | C.I. Reactive Orange 16 | | | | | | | | 156 | |
| Brazilian pine-fruit shells | C.I. Reactive Black 5 | Batch | 30<br>40<br>50 | 2 | 4 | n/a | 100 | 720 | 55.6<br>64.8<br>74.6 | [Cardoso et al., 2011c] |

**Table 3**

Absorption of reactive dyes by chitosan and chitosan derivatives

| Ion-exchange resins | Dye type | Treatment methods | Operating conditions | | | | | | Dye binding capacity (mg $g^{-1}$) | Ref. |
|---|---|---|---|---|---|---|---|---|---|---|
| | | | Temperature of treatment (°C) | Optimum pH | Dosage of sorbent (g $l^{-1}$) | Agitation speed (rpm) | Dye conc. (mg $l^{-1}$) | Contact time (min) | | |
| Chitosan alone | | | | | | | | | | |
| Commercial chitosan powder | Reactive Black 13 | Batch | 30 | 6.7 | 10 | n/a | 200 | 20 | 91.5 | [Jiang et al., 2014] |
| Chitosan bead | C.I. Reactive Red 189 | Batch | 30 | 1<br>9 | 2 | n/a | 3768 | 7200 | 1189.0<br>756.0 | [Chiou and Li, 2002] |
| Chitosan | C.I. Reactive Red 3 | Batch | 20 | | 1.2 | 400 | 100 | 1440 | 81.4 | [Filipkowska, 2006] |
| Chitosan | C.I. Reactive Black 5 | Batch | 25<br>45<br>65 | 2 | 1 | 160 | 300 | 1440 | 224.0<br>284.0<br>345.0 | [Nga et al., 2017] |
| Squid pen | C.I. Reactive Green 12 | Batch | 20 | n/a | n/a | 100 | 180 | 21600 | 202.00 | [Figueiredo et al., 2000] |
| Chitosan powder | C.I. Reactive Red 198 | Batch | 25 | 4 | 0.5 | 175 | 80 | 360 | 1250.0 | [Subramani and Thinakaran, 2017] |
| Chitosan film | C.I. Reactive Blue 19 | Batch | 20 | 6.8 | n/a | 150 | 1000 | 150 | 799.0 | [Chiou et al., 2004] |
| Chitosan derivatives | | | | | | | | | | |
| Porous chitosan-polyaniline/ZnO hybrid composite | Reactive Orange 16 | Batch | 37±0.2 | 3 | 1 | 100 | 50 | 60 | 476.2 | [Kannusamy and Sivalingam, 2013] |
| ECH crosslinked chitosan nanoparticles | Reactive Black 5<br>Reactive Orange 16 | Batch | 30 | 2 | 0.9 | n/a | 8000 | 9600 | 5572.0<br>5392.0 | [Chen et al., 2011] |
| ECH crosslinked chitosan bead | C.I. Reactive Red 189 | Batch | 30 | 1 | 2 | n/a | 3768 | 7200 | 1642.0 | [Chiou and Li, 2002] |

| | | | | | | | | | | |
|---|---|---|---|---|---|---|---|---|---|---|
| ECH-crosslinked chitosan beads | Reactive Blue 2 | Batch | | 3 | | | | | 2498.0 | [Chiou et al., 2004] |
| Chitosan X-linked by sodium edetate | Reactive Black 5<br>Reactive Yellow 84 | Batch | 20<br>60 | 4 | 1 | 150 | 200-4000 | 336 | 1025.6<br>1539.7 | [Jóźwiak et al., 2015] |
| X-linked quaternised chitosan | Reactive Orange 16 | Batch | 25 | 3 | 1 | 250 | 1000 | 2000 | 1060.00 | [Rosa et al., 2008] |
| 3-aminopropyl 7 triethoxysilane modified chitosan beads | Reactive Blue 4 | Batch | | 4 | 1 | 200 | 500 | 480 | 317.12 | [vakili et al., 2015] |
| Polyethyleneimine-grafted-chitosan hydrogel beads | C.I. Reactive Black 5 | Batch | 30 | 5 | 20 | 150 | 500 | 1440 | 709.3 | [Chatterjee et al., 2011] |
| Polyethyleneimine-grafted-chitosan hydrogel beads with sodium dodecyl sulphate | | | | | | | | | 413.2 | |
| Epichlorohydrin-crosslinked chitosan beads | C.I. Reactive Red 222 | Batch | 30 | 3 | 1 | 100 | 1000 | 1440 | 2252.0 | [Chiou et al., 2003] |
| Chitosan powder grafted with poly(acrylamide) | C.I. Reactive Yellow 176 | Batch | 25 | 2 | 1 | n/a | 100 | 1440 | 928.0 | [Kyzas and Lazaridis, 2009] |
| Chitosan bead grafted with poly(acrylamide) | | | | | | | | | 863.0 | |

**Table 4**

Removal performance of reactive dyes by magnetic nanoparticles

| Adsorbents | Dye type | Treatment methods | Operating conditions | | | | | | Absorption capacity (mg $g^{-1}$) | Ref. |
|---|---|---|---|---|---|---|---|---|---|---|
| | | | Temperature of treatment (°C) | Optimum pH | Dosage of sorbent (g $l^{-1}$) | Agitation speed (rpm) | Dye conc. (mg $l^{-1}$) | Contact time (min) | | |
| Laccase immobilised magnetic chitosan beads | C.I. Reactive Yellow 2 | Batch | 30 | 5.5 | 20 | n/a | 50 | 1080 | 2.05 | [Bayramoglu et al., 2010] |
| | C.I. Reactive Blue 4 | | | | | | | | 1.42 | |
| Magnetic chitosan microparticles functionalised with polyamidoamine dendrimers | C.I. Reactive Blue 21 | Batch | 30 | 6.4 | | 120 | 80 | 720 | 555.56 | [Wang et al., 2015] |
| Magnetic N-lauryl chitosan particles | C.I. Reactive Red 198 | Batch | 25 | 3 | 1.25 | n/a | 500 | 60 | 374.00 | [Debrassi et al., 2012] |
| Quaternised GLA crosslinked chitosan/magnetite nanoparticles | C.I. Reactive Black 5 | Batch | 25 | 3 | 1.11 | 300 | 1938.6 | 180 | 773.60 | [Elwakeel, 2009] |
| Magnetic chitosan nanoparticle | C.I. Reactive Blue 4 | Batch | | 4 | 1 | 200 | 500 | 480 | 433.74 | [Jafari et al., 2016] |
| Modified magnetic chitosan microspheres | Reactive red 120 | Batch | 25± 2 | 7 | 3 | 200 | 3333.33 | 120 | 166.7 | [Li et al., 2014] |
| Magnetic carbon nanotube-κ-carrageenan-$Fe_3O_4$ nanocomposite | C.I. Reactive Black 5 | Batch | 25 | 2 | 0.4 | 150 | 19.84 | 1440 | 22.01 | [Duman et al., 2016] |
| Quaternised magnetic resin microspheres | C.I. Reactive Red 120 | Batch | 20 | 5 | 0.2 | 130 | 669 | 50 h | 1029.0 | [Shuang et al., 2012] |
| | C.I. Reactive Orange 16 | | | | | | 308.8 | | 1173.3 | |

| | | | | | | | | | | |
|---|---|---|---|---|---|---|---|---|---|---|
| O-carboxymethyl chitosan-N-lauryl/c-$Fe_2O_3$ magnetic nanoparticles | C.I. Reactive Red 198 | Batch | 25<br>55 | 2 | 1 | n/a | 250 | 120 | 216<br>390 | [Demarchi et al., 2015] |
| L-arginine-functionalised $Fe_3O_4$ nanoparticles | C.I. Reactive Blue 19 | Batch | 25 | 3 | 0.74 | 250 | 50 | 2880 | 66.66 | [Dalvand et al., 2016] |
| Magnetic $Fe_3O_4$/chitosan | C.I. Reactive Red 2 | Batch | 25± 0.5 | 2 | 0.6 | 180 | 200 | 300 | 476.8 | [Cao et al., 2014] |